



**HAL**  
open science

## Is the Machecoul fault the source of the $\sim$ M6 1799 Vendée earthquake (France)?

C. Kaub, L. Geoffroy, L. Bollinger, J. Perrot, P. Le Roy, C. Authemayou

► **To cite this version:**

C. Kaub, L. Geoffroy, L. Bollinger, J. Perrot, P. Le Roy, et al.. Is the Machecoul fault the source of the  $\sim$ M6 1799 Vendée earthquake (France)?. *Geophysical Journal International*, 2021, 225, pp.2035-2059. 10.1093/gji/ggab076 . insu-03684640

**HAL Id: insu-03684640**

**<https://insu.hal.science/insu-03684640>**

Submitted on 1 Jun 2022

**HAL** is a multi-disciplinary open access archive for the deposit and dissemination of scientific research documents, whether they are published or not. The documents may come from teaching and research institutions in France or abroad, or from public or private research centers.

L'archive ouverte pluridisciplinaire **HAL**, est destinée au dépôt et à la diffusion de documents scientifiques de niveau recherche, publiés ou non, émanant des établissements d'enseignement et de recherche français ou étrangers, des laboratoires publics ou privés.



Distributed under a Creative Commons Attribution 4.0 International License

# Is the Machecoul fault the source of the $\sim M6$ 1799 Vendée earthquake (France)?

C. Kaub,<sup>1,\*</sup> L. Geoffroy<sup>1</sup>, L. Bollinger,<sup>2</sup> J. Perrot,<sup>1</sup> P. Le Roy<sup>1</sup> and C. Authemayou<sup>1</sup>

<sup>1</sup>UMR 6538 Géosciences Océan, IUEM-UBO, Place Nicolas Copernic, F-29280 Plouzané, France. E-mail: [caroline.kaub@hotmail.fr](mailto:caroline.kaub@hotmail.fr)

<sup>2</sup>Département Analyse Surveillance Environnement, CEA, DAM, DIF, 91297 Arpajon, France

Accepted 2021 February 17. Received 2021 February 17; in original form 2020 July 18

## SUMMARY

The  $\sim M6$  1799 Bouin earthquake is considered as one of the largest earthquakes to have struck Western France. However, the seismogenic source potentially responsible for this event remain marginally documented. We present results from a focused offshore-onshore multidisciplinary survey in its meizoseismal area in order to identify the fault segments that potentially ruptured during this earthquake. Based on macroseismic data and the geology, we focused our study on the so-called Machecoul Fault as a potential source of the 1799 Bouin event. Our survey includes extensive high-resolution seismic reflection, high resolution bathymetry and a 1-yr seismological survey. These data were combined with existing topography, onshore gravity data and drill data to document the geometry of the Marais Breton/Baie de Bourgneuf basin, the past tectonic activity and the current local microearthquakes at depth along its bounding faults. Offshore and onshore observations suggest a recent activity of the segmented Machecoul Fault bounding the basin to the North. Offshore, the planar contact between the Plio-Quaternary sediments and the basement along the fault trace as well as the thickening of these sedimentary units near this contact suggests tectonic control rather than erosion. Onshore, the recent incision of the footwall of the fault suggests a recent tectonic activity. The temporary local seismological experiment deployed between 2016 and 2017 recorded a diffuse microseismicity down to the depth of  $22 \pm 5$  km along the southward dipping Machecoul Fault, associated with predominantly normal fault mechanisms. Altogether, these results suggest that the Machecoul Fault is a serious candidate for being the source of the historical Bouin 1799 earthquake.

**Key words:** Europe; Seismicity and tectonics; Intra-plate processes.

## 1 INTRODUCTION

Western Europe is considered as a Stable Continental Interiors (Johnston 1989, or Regions, SCR) because of low deformation rates (e.g. Nocquet 2012; Masson *et al.* 2019) and tectonic processes associated with a very diffuse and weak imprint on geology and topography. Significant earthquakes are infrequent in SCR and may correspond to the triggered release of elastic strain accumulated in the lithosphere on long time scales (e.g. by variations in crustal stress or fault strength if large enough, Craig *et al.* 2016). They can occur in regions devoid of current seismicity (García-Moreno *et al.* 2015) or Quaternary ruptures evidences (e.g. in Western Europe, Audin *et al.* 2002) and are rarely located on well-defined crustal structures (e.g. Calais *et al.* 2016; Stein *et al.* 2017). However, because of the particularly low seismic energy attenuation in intraplate regions (Hanks & Johnston 1992), and in the context of

highly populated regions, shallow depths and intermediate magnitude earthquakes can have devastating and expensive consequences (e.g. 1756 Düren (Germany) or 1356 Basel (Switzerland), Fäh *et al.* 2001; Bilham 2004). Quantification of the seismic hazard associated with SCR earthquakes remains a challenge (e.g. Ellsworth *et al.* 2015; Petersen *et al.* 2015), particularly in intraplate Europe (Stein *et al.* 2017). We focus our study in the Vendée department in metropolitan France, a region known to have been affected by a major devastating earthquake in 1799 ( Figs. 1–A quality and 2). This earthquake is currently considered as one of the largest events which occurred in metropolitan France. It falls in a region classified level 3 (moderate seismicity) on a scale of five levels, according to the latest seismic zoning for normal risk assessment following Eurocode 8 (Zonage Sismique de la France 2011). The seismogenic potential of the faults in the Vendée department needs therefore to be clarified.

\* Now at: SEISTER S.A.S.

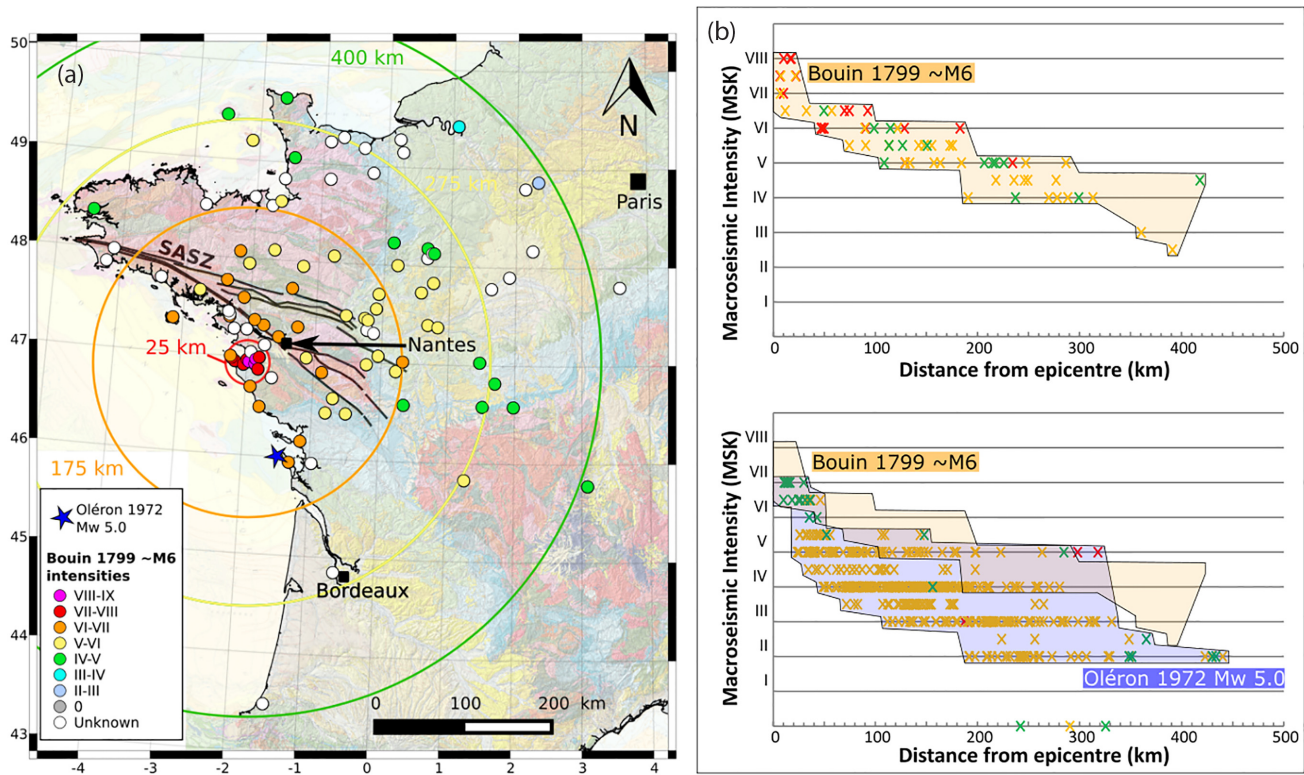


**Figure 1.** Left-hand panel: map representing the regional coverage of Bouin 1799 earthquake macroseismic data (99 point macroseismic MSK-64 intensities (Medvedev *et al.* 1967) deduced from historical accounts and compiled in SisFrance database (<https://sisfrance.irsn.fr/> Scotti *et al.* 2004). The 25, 175, 275 and 400 km radius circles delineates respectively the extent of VII–VIII (in red), VI–VII (in orange), V–VI (in yellow) and IV–V (in green) intensity area respectively (MSK-64). SASZ: South Armorican crustal Shear Zone. Right-hand panel: envelopes of macroseismic intensities for Bouin 1799 and Oléron 1972 (450 accounts) as a function of their epicentral distance. The colours correspond to the qualities of the accounts: A quality (sure intensity) in green, B quality (intensity sure enough) in orange, C quality (uncertain intensity) in red.

The objective of this study is to document the Machecoul Fault's geometry and its short and long-term activity in order to determine whether this fault could be the source of the  $\sim M6$  1799 Bouin earthquake (France). For that purpose, we studied the area both onshore and offshore using a multidisciplinary work based on the acquisition of an extensive high-resolution seismic survey (Sparker source and single channel streamer, CHIRP echo sounder) and high resolution bathymetry data (GeoSwath), compared with onshore drilling data (BSS, BRGM), topography data (RGEALTI) and onshore gravity data (BGI). This analysis documents the geometry and potential syn-tectonic nature of the neogene sedimentary infilling of the thin Marais Breton/Baie de Bourgneuf basin and tests if the Machecoul Fault, at the northern edge of the basin, was active after the Eocene (see hereafter, geological setting). We further analysed the present-day morphology of the NW–SE trending Machecoul Fault escarpment to decipher its potential tectonic signal. A temporary local seismological experiment of 10 stations was also deployed between 2016 and 2017 to record and characterize the background seismic activity in the area.

## 2 THE $\sim M6$ 1799 BOUIN EARTHQUAKE (VENDÉE)

The 1799 earthquake, of unknown mechanism, affected the coastal Vendée and the Nantes area just before 4:00 a.m. on January 25th (Publicateur de Nantes, 1 Ventôse an VII, that is 1799 February 19, in Limasset *et al.* 1992). The main shock was widely felt in

metropolitan France, in the far field up to 435 km in Central Massif (Fig. 1a, SisFrance, <https://sisfrance.irsn.fr/>, last accessed on July 2020), attesting for its significance in term of seismic source (its magnitude is estimated around  $\sim M6$ ). Baumont & Scotti (2011) determined a macroseismic hypocentre (46.967N 2.1W, depth of 24 km) associated to an epicentral intensity  $I_0$  VII–VIII (MSK-64) and a macroseismic Moment Magnitude  $M_w$   $6.33 \pm 0.28$ . Stucchi *et al.* (2013), with the same input, obtained a macroseismic  $M_w$   $5.63 \pm 0.22$ . The SHEEC-SHARE european catalogue gives a macroseismic  $M_w$   $6.16 \pm 0.3$  which corresponds to the weighted average of the Stucchi *et al.* (2013) and the Baumont & Scotti (2011) magnitudes. Finally, Manchuel *et al.* (2017) adopted the Baumont & Scotti (2011) epicentre and determined a macroseismic  $M_w$   $6.30 \pm 0.34$  and a depth of 21 km. Note that all the macroseismic focal depths obtained are significantly larger than the 11–13 km usually determined for the recent earthquakes that occurred in the Armorican Massif (Mazabraud *et al.* 2005; Perrot *et al.* 2005).

Despite less documented intensities below V (MSK-64) due to a poorer documentation of the accounts and a probably higher building vulnerability in 1799 than during the late 20th century, the macroseismic intensities show some similarities with the ones documented after the 7 September 1972 in Oléron earthquake ( $M_w$  Si-Hex 5.0, Cara *et al.* 2015), a significant event felt up to 440 km (Fig. 1b, SisFrance). Effects and damages for this later event are well documented. This event is currently the largest instrumental earthquake documented by the national seismological network along the Atlantic coast. Compared to the 1799 Bouin event, the Oléron earthquake shows a larger scattering of macroseismic

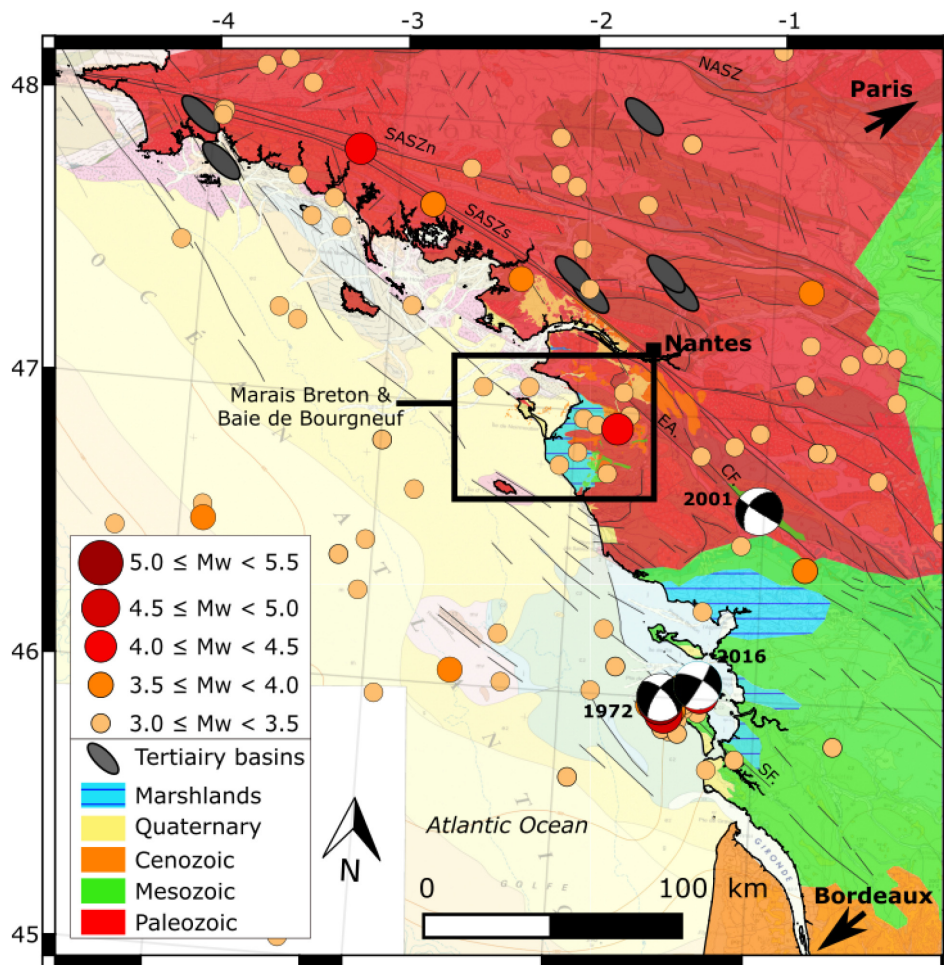


**Figure 2.** Simplified geological map of western France and available seismicity from 1962 to 2017 (Si-Hex and CEA-LDG catalogues). We homogenized magnitudes following the Cara *et al.* (2015) conversions. The area of study is located in the black rectangle. The focal solutions correspond to the three instrumental earthquakes Oléron 1972  $M_w$  Si-Hex 5.0, Chantonnay 2001  $M_w$  Si-Hex 3.7 and La Rochelle 2016  $M_w$  Si-Hex 4.4 (Nicolas *et al.* 1990; Duverger *et al.* submitted). Thin black lines are regional faults from the 1:1 million geological map of France. SASZs and SASZn: South Armorican crustal Shear Zone south and north. NASZ: North Armorican crustal Shear Zone. EA: Essarts Accident. CF: Chantonnay Fault. SF: Seudre fault.

intensities relative to the epicentral distance, reaching 1.5 degree of intensity (Fig. 1b). This could be partially due to the heterogeneities coming from source radiation, the seismic waves path, local sites effects and/or variable building vulnerability as well as from a better reporting. The mesoseismal area for the Bouin event includes the Marais Breton basin where maximum intensities up to VIII–IX (MSK-64) were reached (Fig. 1a, SisFrance). The swampy Marais Breton basin is probably prone to seismic wave amplification and liquefaction due to the nature of the unconsolidated sedimentary layers and the presence of shallow water (Rey *et al.* 2016). Intensities greater or equal than VII–VIII (MSK-64) were reached within a 25 km radius coastal area including the Machecoul, Noirmoutier and Bouin localities.

The macroseismic magnitudes and depths determined for the 1799 earthquake rely on the epicentral location of Baumont & Scotti (2011, FPEC catalogue). The macroseismic epicentre initially determined as the barycentre of the isoseismals of maximal intensities (Scotti *et al.* 2004) falls into the Baie de Bourgneuf (Bourgneuf Bay). A 20-km-large radius of uncertainty was assigned to this epicentre, leading the possibility that the earthquake occurred in the Baie de Bourgneuf, in the Marais Breton, or their immediate vicinity. The actual epicentre most probably falls in that region.

Indeed, this area is intersected by a circle of  $\sim 32$  km of radius centred on Nantes. These 32 km correspond to the probable hypocentral distance to Nantes, where Blin 1799 (see Limasset *et al.* 1992) reported a delay of 4 s between two distinct shocks interpreted here as  $P$  and  $S$  arrivals from which the hypocentral distance was deduced.

Several faults are situated within 20 km from the macroseismic epicentre, including the Noirmoutier and Machecoul Faults (Fig. 3). Accounts of submersion linked to landslides and beaver dam failures described in Bourgneuf-en-Retz and Nantes harbours (Fig. 3) led Limasset *et al.* (1992) to argue in favour of an offshore epicentre on the continental shelf. Thus, excluding the onshore faults previously described in the coastal Vendée area (e.g. Ters *et al.* 1979a,b, 1983), Limasset *et al.* (1992) proposed that the 1799 seismic rupture could be associated with a southeastward offshore extension of the Noirmoutier Fault. However, the occurrence of an earthquake felt only in Machecoul village a few hours before the main shock at around 00:30 a.m. is also known (Publicateur de Nantes, 1 Ventose an VII, that is 1799 February 19, in Limasset *et al.* 1992), whereas no account of this event is recorded elsewhere in the mesoseismal area, which remains well-documented by the early chronicles which covered the event (Limasset *et al.* 1992). These elements favour the Machecoul Fault as the origin of the 1799 earthquake. Indeed, up

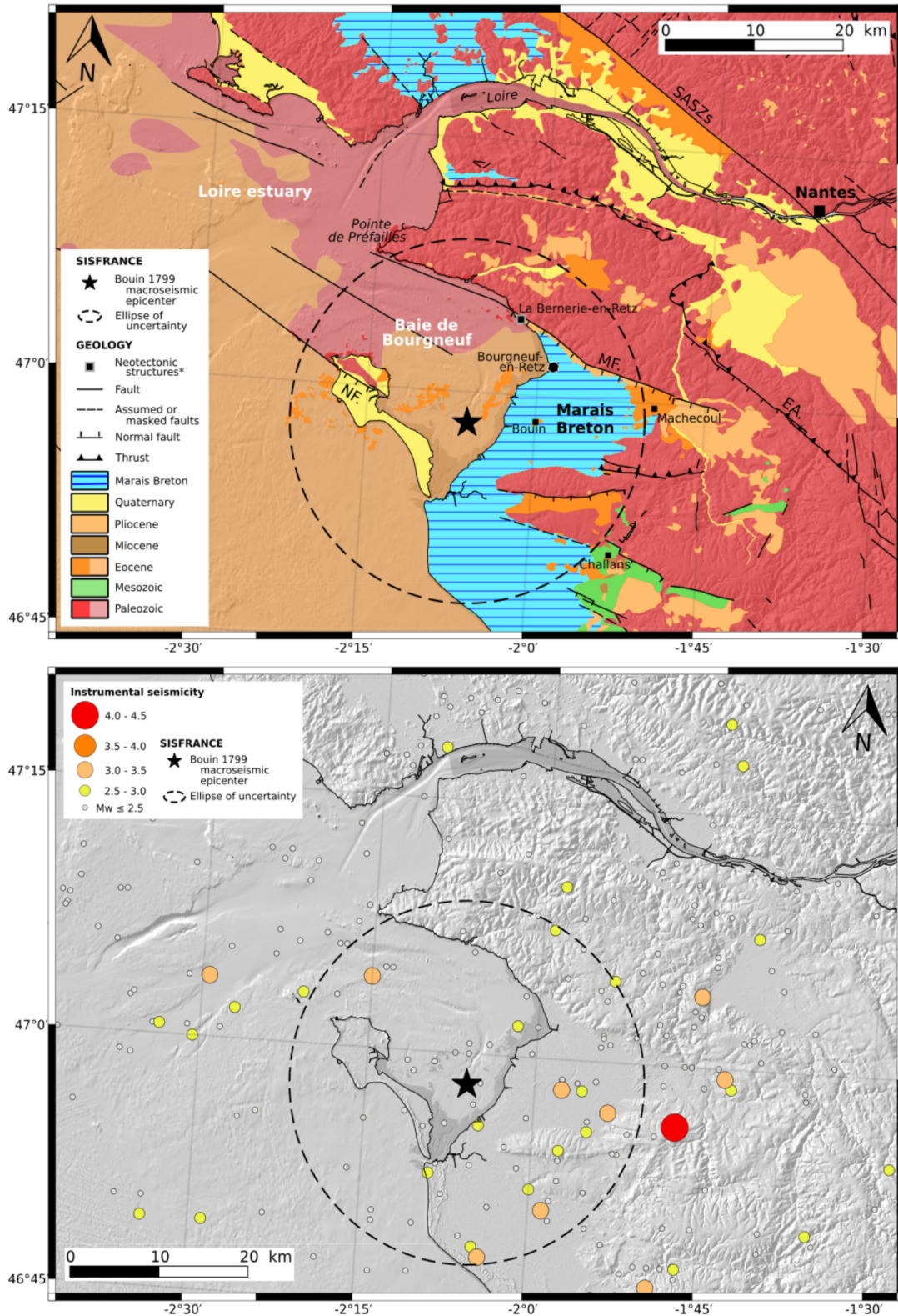


**Figure 3.** Simplified geological map of coastal Vendée (top panel) and seismological data available from 1962 to 2014 (Si-Hex and CEA-LDG catalogues, bottom panel). The SISFRANCE macroseismic epicentre of the 1799 Bouin earthquake and its 20 km ellipse of uncertainty are represented (SisFrance, <https://sisfrance.irs.fr/>). The location of the neotectonic structures in La Bernerie-en-Retz, previously described by Baize *et al.* (2002) is specified (see text and Appendix Fig. D1). MF: Machedoul Fault. NF: Noirmoutier Fault. EA: Les Essarts Accident. SASZs: South Armorican crustal Shear Zone south.

to 70 per cent of M6 earthquakes inland are preceded by foreshocks (e.g. in Reasenber [1999](#); Tamaribuchi *et al.* [2018](#)), events that generally occur on the fault at failure during the main shock. The very low rate of felt earthquakes in the Marais Breton suggests that the event felt in the village of Machecoul, 3 hr before the main ~M6 Bouin earthquake is related to the latter.

### 3 GEOLOGICAL AND SEISMOLOGICAL SETTING

#### 3.1 Geological setting

The study area is located in the southern part of the Armorican Massif and south of the NW–SE trending South Armorican crustal Shear Zone (SASZ, Ballèvre *et al.* [2009](#)), the major Variscan structure of the region ( Figs. 2 and 3). This intraplate geological region is affected by a system of dominantly NW–SE and NNW–SSE trending basement faults inherited from a long and polyphased tectonic history since Variscan times, reactivated several times notably during the Mesozoic and Tertiary (e.g. Vignerresse [1988](#); Bonnet *et al.* [2000](#); Truffert *et al.* [2001](#)). Several of the fault segments were also considered as reactivated syn- to post- Pliocene or during the Quaternary (see Jomard *et al.* [2017](#), and references therein). This is not an unique case in Brittany: indeed, Quaternary activity was also described in Crozon Peninsula where basement faults were reactivated during Pleistocene palaeo-earthquakes (Van Vliet-Lanoë *et al.* [2018](#)). Reactivated faults during the Quaternary have been debated close to the north of the Loire estuary, that is to the north of our studied area (Fig. 3, Brault *et al.* [2001](#); Van Vliet-Lanoë *et al.* [2009](#)). Some of these faults bound tertiary onshore and offshore basins (e.g. Jaeger [1967](#); Delanoë [1988](#); Borne *et al.* [1991](#); Wyns [1991](#); Guillocheau *et al.* [2003](#); Bessin *et al.* [2015](#)). The N110–130° trending Machecoul Fault belongs to this fault's family. It bounds an extensive Holocene marshland, the Marais Breton, and its marine extension the Baie de Bourgneuf basin ( Figs. 2 and 3). Southward along the Atlantic coast, several Holocene low-lands appear to be partly controlled by basement discontinuities trending WNW–ESE such as the Marais Poitevin and the Perthuis Breton basins and the Marais de Marennes – Rochefort-sur-Mer and the Perthuis d'Antioche basins (Fig. 2, Wyns [1986](#)). The Machecoul Fault was formerly described as a “large littoral fault along the [Baie de Bourgneuf northern] cliffs” (Gautier [1969](#)), ‘showing a rectilinear scarp of N110° general direction’ and was interpreted as the southwestern boundary of a northeastward tilted basement block (Ters *et al.* [1979a, 1982](#); Sellier [2015](#)). Faults in the regional geological maps are deduced from morphostructures (lineaments) and from cartographic evidences (e.g. basin/basement tectonic-type contact). Major shear zones such as the SASZ may be interpreted from the few available crustal-scale seismic lines (Bitri *et al.* [2010](#)).

The basement of the Marais Breton and Baie de Bourgneuf area crops on the footwall of the Machecoul Fault, and is mainly composed of magmatic and metamorphic rocks of variscan age. A very thin and local Cenozoic sedimentary cover locally overlays it (Fig. 3). Variscan basement outcrops are also visible offshore in the Loire estuary and in the northern and western parts of the Baie de Bourgneuf (Fig. 3). Mesozoic sediments are almost absent from the southern emerged part of the Armorican Massif but are locally preserved onshore south of our study area (Barrois [1921](#); Durand [1960](#); Béchenec [2009, 2007](#)). Eocene deposits are widespread onshore and offshore south of the Machecoul Fault (Fig. 3, Borne *et al.* [1989](#)) and Oligocene deposits are missing in the Marais

Breton (e.g. Delanoë [1988](#)). Neogene formations are represented by Miocene local deposits to the south of coastal Vendée while sandy Pliocene deposits are widely presents in the vicinity of the Marais Breton, and overlying the basement or the Eocene formations (Fig. 3, Gautier [1962, 1969](#)).

The Baie de Bourgneuf, south of the coastal estuary of the Loire River, is partially closed southwestward by the Noirmoutier barrier Island (Fig. 3). This bay was formed at the end of the last ice age when the rising sea invaded low-lying coastal river valleys (Proust *et al.* [2010](#)). It is incised by current SE–NW oriented channels. The extensive ancient fluvial network in the present day Loire River estuary is known since Vanney ([1964](#)) and was mapped by Thinon *et al.* ([2008](#)). Its sedimentary infilling was characterized by Proust *et al.* ([2010](#)). The substratum of the valleys is composed of discordant Eocene sediments on top of the Variscan basement (e.g. Delanoë *et al.* [1976](#); Huerta *et al.* [2010](#); Menier *et al.* [2014](#)). The sedimentary coastal wedge of the Loire River is non-uniformly preserved in the palaeovalley network and constitutes an exceptional long-term record probably extending from late Bartonian to early Pleistocene, including potentially several erosional events (Proust *et al.* [2001](#); Menier *et al.* [2006a](#)). The palaeovalley network and its infilling in the Baie de Bourgneuf still need to be studied. However, it is known that the seafloor sediments composition is mostly muddy (Delanoë *et al.* [1976](#)) and coarse-grained around basement rocky outcrops (Gouleau [1968](#); Lesueur & Klingébiel [1986](#)). Geological evidences such as Variscan basement outcrops suggest that the overall sediment thickness is small (Fig. 3).

#### 3.2 Seismological setting

The Armorican Massif presents a diffuse seismic activity potentially related to the local reactivation of inherited structures affecting the basement. Together with this diffuse activity, local seismic clusters were observed along the SASZ following moderate earthquakes (e.g. Perrot *et al.* [2005](#)). In addition to the 1799 earthquake, the most damaging historical events of the Armorican Massif happened in Ste-Maure-de-Touraine (15/02/1657), Loudun (06/10/1711) and Parthenay (09/01/1772,  $I_0$  VII–VIII MSK-64 for both in Scotti *et al.* [2004](#)). Two moderate events of the early 20th century (locally damaging,  $I_0$  VII) were documented by both macroseismic observations and early instrumental records, the January 9th 1930 north of Vannes, and the Quimper earthquake of 2 January 1959 ( $M_w$  5.2 and 5.4, respectively, Cara *et al.* [2015](#)). Since then, no earthquake exceeded the intensity VI. Despite that, our knowledge of the local seismicity has been considerably improved since the deployment of the national seismological network in 1962. Since then, thousands of small earthquakes were located all over Brittany, though more densely along the SASZ at midcrustal depths. During this period, a moderate but regular background instrumental seismic activity was documented in the Marais Breton and vicinity, culminating with an earthquake of  $M_w$  Si-Hex 4.1 in 1968 ( Figs. 2 and 3, red circle). This event probably happened close to the historical earthquakes of Bourgneuf-en-Retz (07/04/1767,  $I_0$  VI MSK-64 in Baumont & Scotti [2011](#)) or Bouin 1799. South of the SASZ, in a local tectonic and sedimentary setting and a stress field probably similar to those of the Marais Breton, three significant instrumental earthquakes affected the coastal area from Nantes to Bordeaux (Oléron 1972  $M_w$  Si-Hex 5.0, Chantonay 2001  $M_w$  Si-Hex 3.7 and La Rochelle 2016  $M_w$  Si-Hex 4.4, Fig. 2). Most of the events are characterized by focal mechanisms ranging from pure/oblique extension to dextral strike-slip (Nicolas *et al.* [1990](#); Mazabraud *et al.* [2005, 2013](#); Duverger

*et al.* submitted; Mazzotti *et al.* submitted). The local orientation of the stress field is primarily attributed to the Africa–Eurasia convergence and the mid-Atlantic ridge push and/or to local variation in rheology favouring stress perturbation (Mazabraud *et al.* 2005, 2013; Perrot *et al.* 2005). It is unclear if body forces associated to glacio-isostatic adjustment (e.g. Nocquet 2012) play any role in the stress field.

## 4 METHODOLOGY

The Machecoul Fault bounds an onshore-offshore basin, so we performed a multidisciplinary analysis (Fig. 4). We analysed a Lidar DEM (RGEALTI) using quantitative geomorphology and we acquired new high resolution bathymetric data (Kaub *et al.* 2017) to better describe the Machecoul Fault and to study if there is a recent relief rejuvenation associated with the fault motion. We used existing gravity data (BGI, <http://bgi.obs-mip.fr/fr>) combined with a drilling database (BSS, BRGM, <http://infoterre.brgm.fr/page/banque-sol-bss>) and we led two new offshore seismic reflection surveys (Le Roy *et al.* 2016; Kaub *et al.* 2017) in order to determine the geometry and infilling, respectively, of the onshore and offshore Marais Breton/Baie de Bourgneuf sedimentary basin. This analysis was complemented by the deployment of a temporary seismological survey dedicated to characterize the hypocentral locations and focal mechanisms of the local seismicity at depth, below the fault system in order to characterize the seismicity at depth and its eventual relation with locked or seismogenic fault segments.

### 4.1 Marine surveys

We investigated the offshore fault segments geometry, and the sediment infilling in the Baie de Bourgneuf, using high-resolution low-penetration offshore seismic data and high-resolution interferometric sonar bathymetry data. Those data were obtained during the RETZ 1 (Le Roy *et al.* 2016) and RETZ 2 (Kaub *et al.* 2017) campaigns operated on the French oceanographic launch Haliotis.

A total coverage of 40 km<sup>2</sup> of high-resolution bathymetry data along the presumed offshore extension of the fault was acquired with a Geoswath interferometric sonar (Fig. 4). Bathymetric profiles were processed (gain filter, tidal correction, false probes automatic filtering and gridding) using CARAIBES©software (developed by IFREMER). We then merged our 2 m planar resolution DEM with a bathymetric DEM of similar resolution from the previous POP-CORE 2016 cruise (Baltzer 2016).

A total of 700 km of high-resolution seismic profiles were acquired using a single-channel (SIG©) streamer and a SPARKER source (Fig. 4). Data were recorded by a DELPH acquisition system©. Sub-bottom profiler (Chirp echo sounder) data were also acquired simultaneously. Sparker seismic lines were processed using the software DELPH interpretation©and Chirp seismic data using the SUBOP©software (developed by IFREMER). All seismic lines were visualized, correlated and interpreted with the Kingdom Suite software (Seismic microtechnology INC©). They are displayed in two-travel time in millisecond (ms). For the time-to-depth conversion, a velocity of 1600 m s<sup>-1</sup> was used for unconsolidated sediment. The seismic data interpretations were done following the seismic stratigraphy principles (Mitchum *et al.* 1977). Lithologic and chronostratigraphic attributions of seismic units are based on previous studies of the south-armoric platform (e.g. Delanoë *et al.* 1976; Menier 2004; Huerta *et al.* 2010; Proust *et al.* 2010). They are mostly speculative because they could not be complemented by

appropriate *in situ* drilling. Four seismic units bounded by unconformities were identified over the seismic basement and described according their acoustic facies variability. They are assumed to correspond to sedimentary deposits according the relative continuous inner reflectors (see 5.2.2 section and appendix A for facies description and raw data). We identified locally the top of the rocky basement characterized by chaotic seismic facies and a very irregular top surface. The sedimentary thickness corresponding to Neogene to Quaternary deposits was thus deduced from the time-to-depth conversion of the whole seismic units located between the basement and the seabed. The maximum penetration of seismic waves is about 50 ms two-travel time and corresponds to a depth ranging from 37.5 to 50 m assuming seismic velocities ranging from 1500 to 2000 m s<sup>-1</sup> in unconsolidated sediments.

### 4.2 Drill holes and gravity onshore data

To extend the sediment infilling data set and to better constrain the basin geometry, we used onshore gravity data from the Bureau Gravimétrique International (BGI) and onshore drilling data from the French national drill holes database (Banque du Sous-Sol – BSS) both available online (Fig. 4).

We computed the complete Bouguer gravity anomaly from the free air anomaly provided by the BGI (Fig. 4). Topography and bathymetry were discretized in parallelepipeds of 90 and 100 m wide, respectively. We assumed for the Bouguer correction a density for the terrain and the seawater of 2670 and 1027 kg m<sup>-3</sup>, respectively. The calculation of the gravity effect of each parallelepiped was made with the Blakely (1995) method. We also used a gravity modelling approach to study the thickness of the local infilling in the vicinity of the Machecoul Fault.

In parallel, we selected 190 drill holes from the BSS database, supplemented by geological cross-sections and/or simplified lithostratigraphic columns along the wells. When this was possible, we selected three key horizons corresponding to the top of the Palaeozoic basement, the top of the Palaeogene formations and the ground surface. From those data we inferred the Neogene to Quaternary sediment thickness.

### 4.3 Seismological survey

We used the seismic bulletins and waveforms from two seismological networks deployed from 2011 to 2015, VENDE and LRYON networks (Fig. 4), respectively set up for a period of 20 months between July 2011 and February 2013 and for 33 months between March 2013 and December 2014. We additionally deployed for the purpose of the study a network of 10 stations around the Baie de Bourgneuf and the Marais Breton basins (MACHE network Fig. 4) to conduct a micro-earthquake monitoring survey from January 2016 to October 2017 in order to locate and provide magnitudes and focal mechanisms of local earthquakes in the vicinity of the Machecoul Fault. We used REFTEK 130B-01/3 dataloggers and short period Lennartz Le3D sensors with a lower cutoff frequency of 1 Hz (sampling rate: 125 Hz). Automatic detections of events were processed by a standard STA/LTA (Short Term Average/Long-Term Average, e.g. Allen 1978) trigger algorithm procedure for the whole continuously recording raw data set. After extraction of waveforms around detection time, events were read, picked and located within the SEISAN software (Havskov & Ottemöller 1999). We picked *P* and *S* first arrivals for 58 events around the Marais Breton and computed hypocentre location using the locator HYPOCENTER

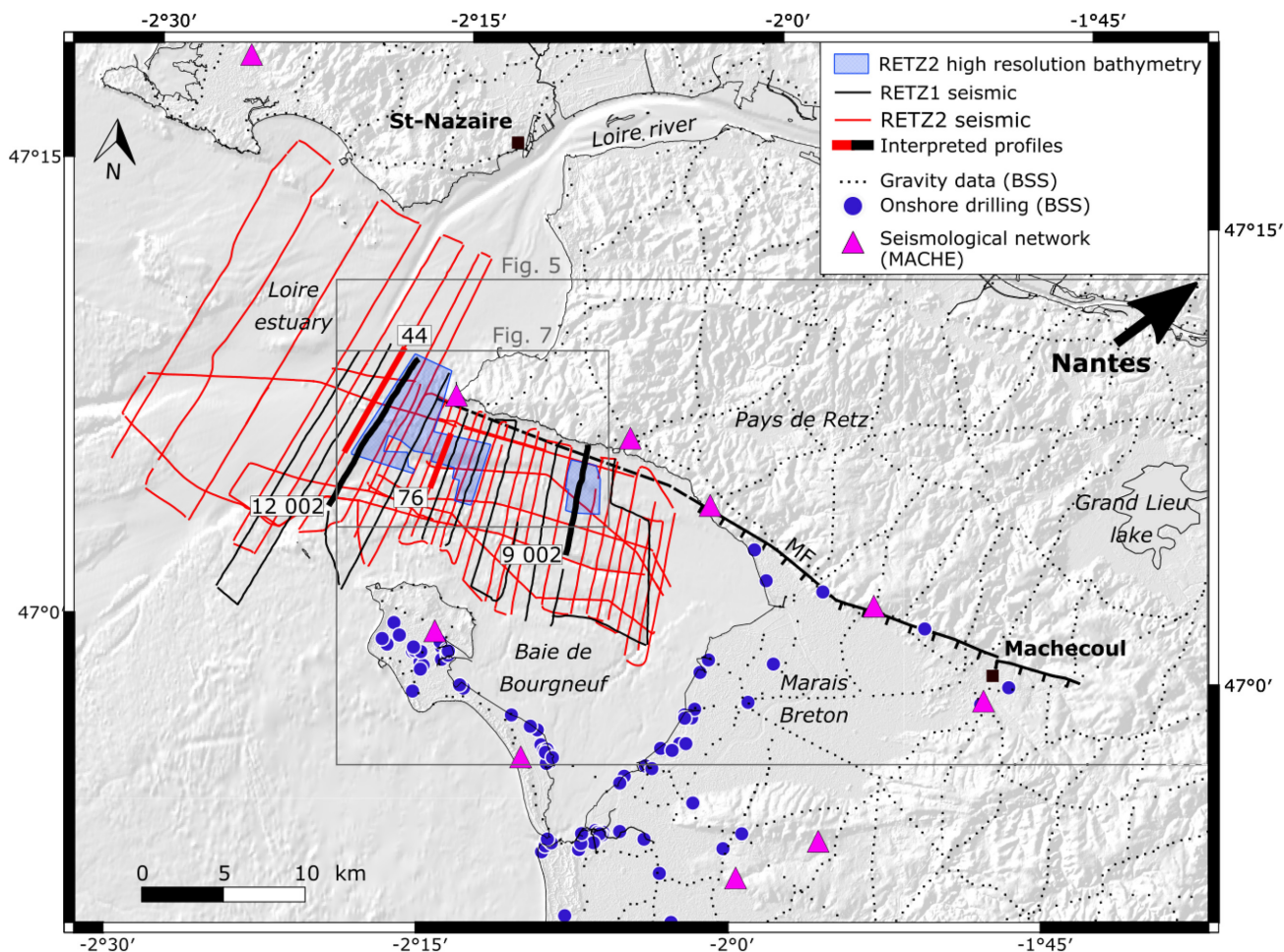


**Figure 4.** Location map of our offshore–onshore surveys (the topographic shaded background corresponds to a digital terrain model from RGEALTI and HOMONIM data bases). Seismic profiles acquired offshore in the Baie de Bourgneuf and Loire estuary during RETZ1 survey (Le Roy *et al.* 2016) and RETZ2 survey (Kaub *et al.* 2017) are in black and red lines, respectively. The 4 interpreted profiles presented in this paper are red and black bold lines. Areas with bathymetric data (RETZ2, Kaub *et al.* 2017) along and across the fault scarp are blue boxes. Used BSS onshore drilling are blue circles. Seismological MACHE network stations are pink triangles (10 stations). Onshore existing gravity data from BGI are small black dots. Figs. 5 and 7 frames are shown. MF: Machecoul Fault.

(Lienert *et al.* 1986). We identified and excluded blast events and regional/global earthquakes from our database. Velocity structure is poorly determined in our study area, so we used the following 4 plane-layered (1-D) crustal velocity model in the location calculations:  $V_p = 5.9 \text{ km s}^{-1}$  from 0 to 14 km depth,  $V_p = 6.5 \text{ km s}^{-1}$  from 14 to 30 km depth and  $V_p = 8.0 \text{ km s}^{-1}$  from 30 to 300 km depth. The bottom of the model is a half-space layer with a velocity of  $V_p = 8.5 \text{ km s}^{-1}$ . This model is based on the work of Arroucau (2006) and Haugmard (2016) on the larger scale of the whole Armorican Massif. Because of the limited extent of our network, the depth of the Moho discontinuity is not decisive and mostly direct rays from the hypocentre to the surface are considered ( $P_g$  and  $S_g$  phases). The  $V_p/V_s$  ratio is assumed to be constant with a value of 1.72.

Coda magnitudes were calculated based on the signal-duration formula of Lee *et al.* (1972). Local magnitudes ( $M_L$ ) were determined following the original Richter (1935) methodology from the amplitude of the  $S$  wave, taking into account the simulation of a Wood-Anderson seismograph generated thanks to the instrument response processed from the PDCC©3.8 software (Casey & DMC 2012) and computed using the Hutton & Boore (1987) formula. First arrival polarities picked were highly uncertain for most of

the 58 micro-earthquakes recorded at the network. To determine focal mechanisms, we focused on the 10 events located inside the network, for which the azimuthal gaps were the smallest (ranging from  $102^\circ$  to  $232^\circ$ ). Fault plane solutions were produced using FP-FIT (Reasenber & Oppenheimer 1985) only for events with more than six polarities which was the case for 8 of the 10 events inside the network. We then used the resulting focal solutions in order to determine a stress tensor solution using the inversion method of Vavryčuk (2014).

#### 4.4 Onshore geomorphological analysis

To investigate if the long-term Machecoul Fault activity could have affected landscape morphology and hydrographic network, we performed a geomorphological analysis with the RGEALTI 5 m DEM of the studied area. We extracted automatically channel networks using RiverTools software (Peckham 2003) from the DEM and we produced an incision map of the region. We detected drainage anomalies as stream deflections on the drainage network or knick-points along the river longitudinal profile (e.g. Whipple & Tucker 1999). The incision map (or ‘geophysical relief’, Ahnert 1984)

corresponds to the difference between an envelope surface (i.e. an imaginary topographic surface tangent to the ridge crests, Bullard & Lettis 1993) and the current topography (Small & Anderson 1998; Brocklehurst & Whipple 2002; Burbank & Anderson 2011). We re-constructed the envelope surface interpolating the high points and the main interflaves of the DEM. The incision map yields minimum values because undissected surface remnants are not present everywhere and interflaves are arbitrarily considered to be uneroded. To better evaluate the incision of the escarpment fault, we realized a swath profile of the footwall parallel to the Machecoul Fault and we document the geometry of six catchments (A to F) distributed alongside the fault trace.

## 5 RESULTS

### 5.1 Morphology of the Machecoul Fault system

The onshore topographic signature of the Machecoul Fault is a very tenuous and highly anthropized (e.g. crosscutting roads, habitations, marshlands) 20-km-long slope break. It separates the Marais Breton southward from the Pays de Retz relief to the north (Fig. 5a). The relative height of the fault escarpment varies between 28 and 7 m (Fig. 5c, profiles n°5 and n°8, respectively). The morphological trace diminishes gradually eastward (Fig. 5a, zone C). From Préfailles to Machecoul city, we distinguish seven segments with a N110° direction, except for a central segment forming a relay zone between the linear sea cliff of Préfailles and the Marais Breton basin. Their length ranges from 2.5 to 12.5 km. Onshore, the topographic escarpment is locally well-expressed, especially in zone B where it culminates at elevations above 30 m (Figs. 5a and c in profile n°5). It decreases gradually eastward in the Marais Breton.

The onshore footwall morphology presents a perched and planar horizontal surface with very homogeneous maximum altitude of 45 m and low values of incision (Fig. 5d). Localized incision are globally related to minor streams draining the footwall and connected to the Falleron stream (catchments A to F, Fig. 6a). The hydrographic network organization is generally consistent with the southward slope direction of the fault escarpment and the surrounding tectonic structures, except for the Tenu river. This epigenic catchment flows northward through the Machecoul Fault escarpment, and reflects the antecedence of the Tenu river. In the footwall, the river incision is maximum but without any perturbation of its longitudinal profile. Knickpoints along the river are located upward or downward of the fault trace at confluences or lithological boundaries (Fig. 6b).

In the foreshore area, the basement outcrops intermittently along the shoreline (Figs. 3 and 5a, zone A). Offshore, the extension of the Machecoul Fault in the Baie de Bourgneuf is visible on both the bathymetry and seismic profiles (Figs. 5b, 7 and 8). On the bathymetric profiles, we observed that the height of the escarpment varies randomly laterally. It could be due to spatial variations of rock roughness or marine erosion processes associated with tidal currents (Figs. 5a and b). We do not observe on the seismic profiles the assumed fault at the toe of the cliffs bounding the Baie de Bourgneuf to the north (Fig. 3). The shallow conditions of acquisition did not allow to approach the cliffs enough. Westward the Baie de Bourgneuf, it is clear on the seismic profiles that the fault system is composed of two parallel escarpments in the vicinity of the Pointe de Préfailles (Figs. 5a and b, zone a and profiles n°10 and n°11, and Fig. 8 profile 12 002). The fault trace is discontinuous and sinuous (Fig. 7), in some places strongly expressed up to the

seafloor (Fig. 5b profile n°14) and in others no longer visible under the recent current sedimentary cover (Fig. 5b profile n°15). The substratum morphology delineates channels organized in linear and longitudinal networks following the NW–SE trending fault scarps. The more visible offshore segment is about 7.5 km long (Figs. 5a zone a and 7 zone A).

### 5.2 Basin geometry and infilling regarding the Machecoul Fault

Both onshore and offshore sedimentary basins at the hangingwall of the Machecoul Fault system were studied through geological maps, gravity and drilling data, and seismic reflection profiles. We determined their geometry and the characteristics of their infilling to evaluate the timing and the amplitude of the potential control of the Machecoul Fault on the sedimentation.

#### 5.2.1 The Marais Breton basin

Some large regional structures are identifiable in the Bouguer anomaly map (Fig. 9 A). The most negative anomalies are located in the vicinity of Nantes along the SASZ (–25 mGal) and the most positive ones along the accident of Les Essarts (25 mGal). In the Marais Breton, the Bouguer anomaly values are quite homogeneous, between –5 and 5 mGal. The trace of the Machecoul Fault is clearly visible, especially in the west part of the Marais Breton (Fig. 9b). The negative anomaly (–5 mGal) south of the fault is linked to the sedimentary basin and the contrasting more positive one (1–4 mGal) to the north is associated with the presence of the metamorphic basement (Fig. 2, meta-ignimbrites and micaschists with a density around 2.74, e.g. Gebelin *et al.* 2004). East of the Machecoul Fault, the strongly positive anomaly can be linked to gneissic unit. The lack of data in the Baie de Bourgneuf prevents any detailed interpretation because of artifacts created by the interpolation. Even if the signal is very weak ( $\pm 5$  mGal Bouguer anomaly), there is a good correlation with the overall sediment thickness deduced from the depth of top of the crystalline basement found in the BSS drill-holes at 41 m depth to the north of the Marais Breton (see Appendix Fig. B1 for gravity modelling).

According to the BSS drill-holes data and as expected, there is no evidence of Mesozoic, Oligocene and Miocene deposits in the Marais Breton. The Eocene deposits are overlying the crystalline basement and sediments above them are thus considered as Plio-Quaternary in age. These young sediments are poorly represented or non-existent on the Machecoul Fault footwall and their distribution is heterogeneous on the hangingwall (Fig. 10). We then estimate that their thickness reach a maximum of 20 m along the fault in the littoral zone. In spite of the lack of drill-holes data in the eastward Marais Breton, we can assume that their overall thickness increases both toward the Machecoul Fault and seaward, as Eocene deposits crop out near Machecoul city (Fig. 3).

#### 5.2.2 The Baie de Bourgneuf Basin

Offshore, the northern boundary of the Baie de Bourgneuf basin consists of the coast cliffs. In the vicinity of our high-resolution bathymetry data boxes (Fig. 5a), the superficial marine sediments mostly consist in fine to coarse sands with some muddy areas (Lesueur & Klingébiel 1986). The sedimentary distribution around all the rocky relief is highlighted by tidal currents channeling and sediments accumulation as sandy banner bank (Fig. 7 zone B, Dyer

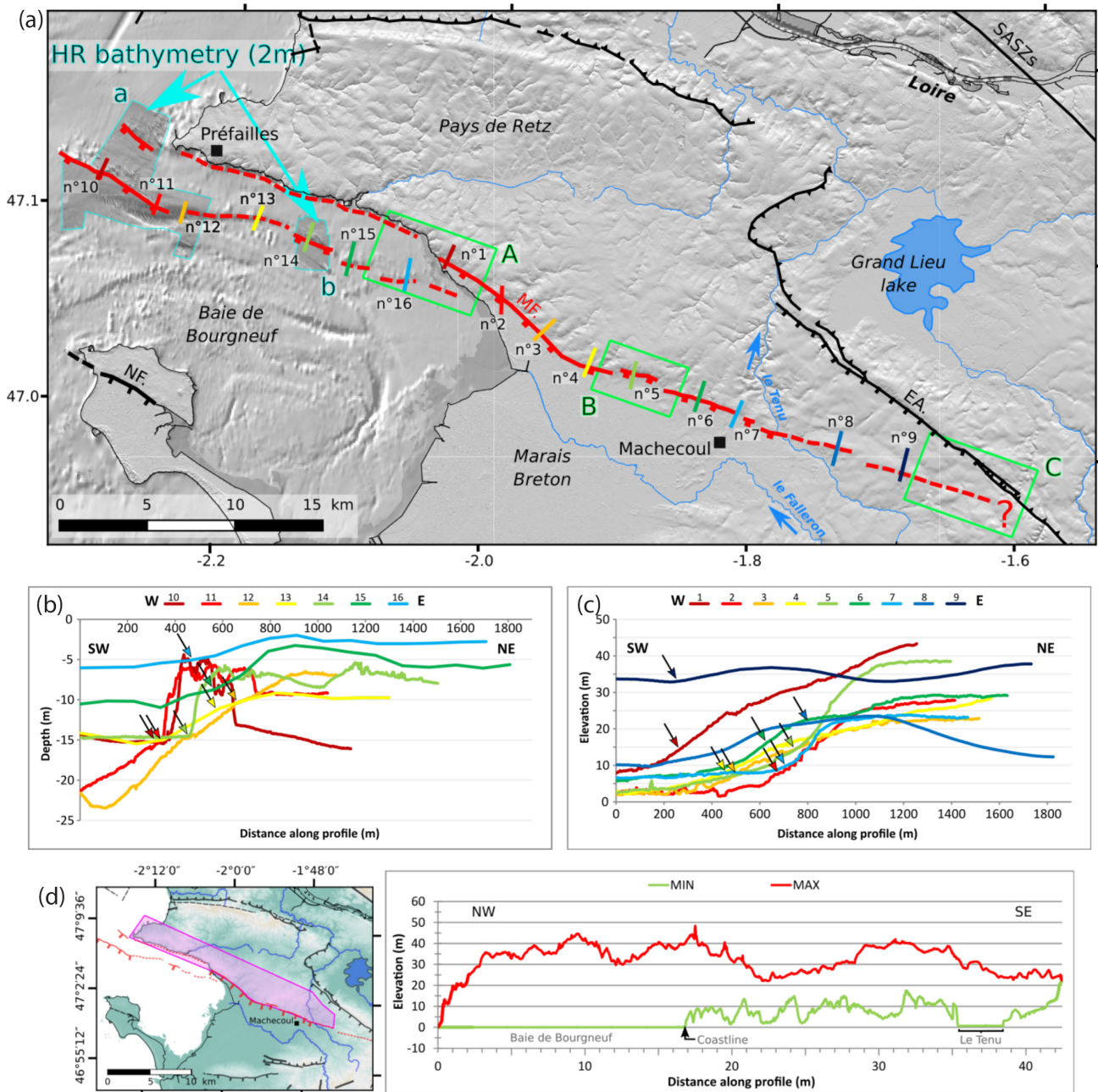


**Figure 5.** (a) Visualization of the fault from shading existing data (RGEALTI 5 m resolution and HOMONIM 100 m resolution respectively, frame on Fig. 4.). The new high resolution bathymetric data acquired during RETZ2 cruise (blue framed, Kaub *et al.* 2017) in the following Fig. 7. Machecoul Fault system (red): slope rupture and marked relief delimiting the structure (solid lines), supposed westward extension of the fault along a less marked topographic scarp (dotted lines). (b and c) Plots of bathymetric profiles 10–16 and topographic profiles 1–9 located on the map on (a). Coloured arrows correspond to the location of the morphological escarpment of the Machecoul Fault on each profile. (d) Swath profiles of the Machecoul Fault footwall relief (pink area on the map). For each point within the swath, minimum (green) and maximum (red) values of elevation along-strike the swath profile are plotted as a function of distance.

& Huntley 1999). Differentiation of the sedimentary facies is limited by the absence of samples and particle size analysis, but 4 seismic units could however be distinguished. We hereafter present a selection of four interpreted seismic profiles representing the variability of our observations from the east part of the Baie de Bourgneuf to the Loire estuary west of our study area (Fig. 8, see Appendix Fig. A3 for facies table description and Figs. A1 and A2 for Sparker and Chirp raw data). The seismic units are chronologically described from the oldest (Us1) to the youngest (U4).

The undifferentiated substratum (Us) is composed of two faulted and deformed seismic units (Us1 and Us2). Its top is incised and delineates the base of a palaeovalleys network (Proust *et al.* 2010). The Us1 basal unit forms the base of almost all the seismic profiles but it is discontinuous. Its inner structure is masked by seafloor reflector multiples. Its upper limit is not strongly marked. It displays a chaotic seismic facies with some steeply inclined reflectors. This unit that locally outcrops at the seabed, is mapped, and corresponds to the magmatic and metamorphic rocks of the South Armorican

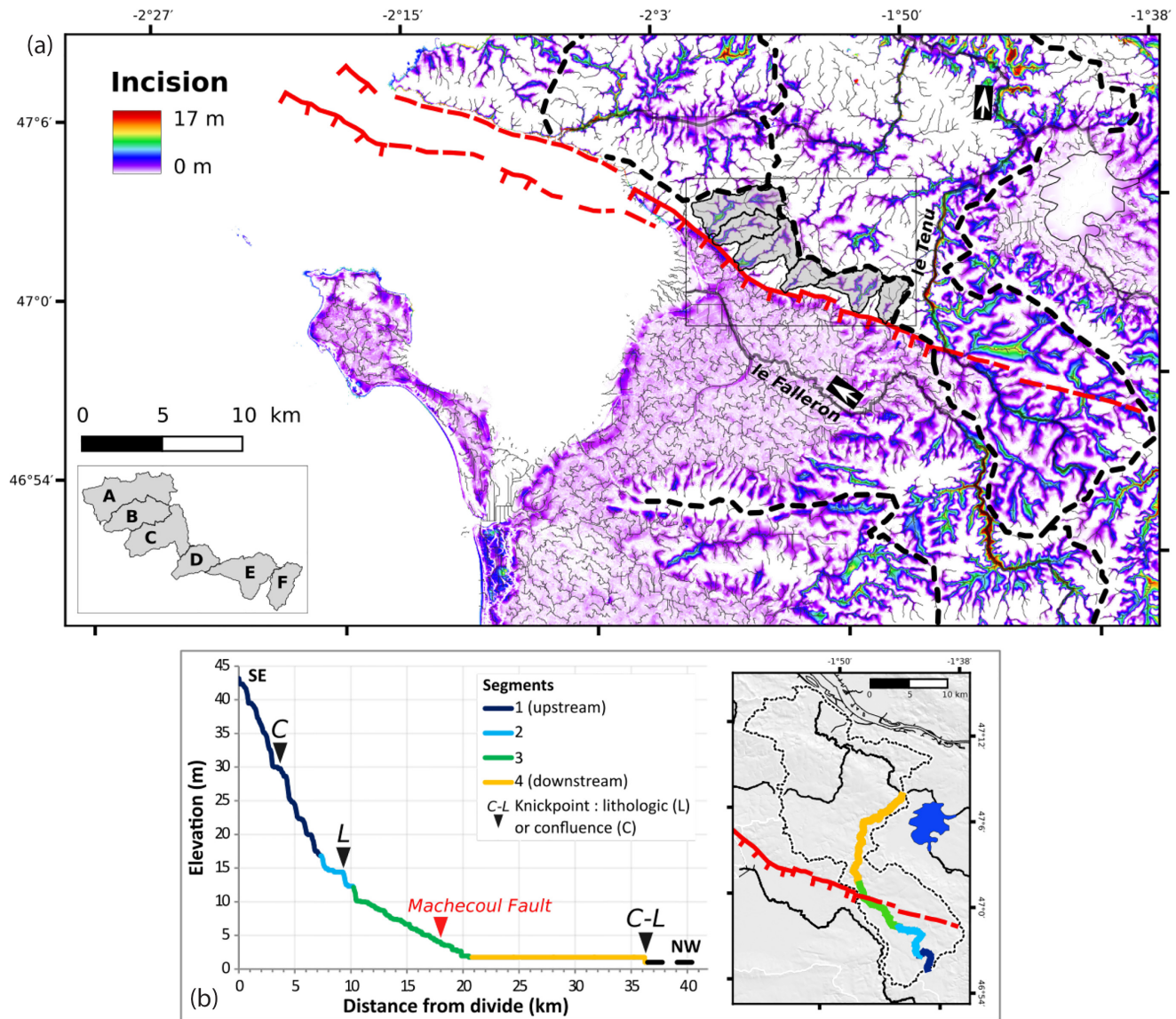


**Figure 6.** (a) Incision map, hydrographic network with main catchments (black dashed lines) and catchments draining the morphological scarp of the Machecoul Fault (grey, a to f from west to east, see also insert map), Machecoul Fault (red). (b) Long profile of Tenu river.

basement. The Us2 unit is limited in its lower part by a truncation surface and flattens the topography by filling the crystalline basement (Us1) depressions (Proust *et al.* 2010). Its top is cut by an erosional surface that delimits the palaeovalleys. It is interpreted as corresponding to the Eocene sandstone-limestone formations, already identified in neighboring areas by Delanoë *et al.* (1976); Menier *et al.* (2006b) and Proust *et al.* (2010). This unit presents laterally a high facies variability, allowing the individualization of two seismic sub-units Us2a and Us2b. The Us2a facies is characterized by chaotic stratification with very low continuity, low frequency reflectors and low to very low amplitudes. This acoustic facies is sometimes transparent. It could be associated with sandstone and terrigenous shell sandstone of Ypresian age (early Eocene, Proust *et al.* 2010). The Us2b facies has a more regular and subhorizontal stratification with low frequency reflectors. The amplitude varies vertically, being stronger in the upper part than in the lower part. This unit is observed mostly faulted, and by place slightly folded (Borne 1986; Proust *et al.* 2001). It could correspond to the bioclastic limestones and sandy limestones of Lutetian and Bartonian ages

(Proust *et al.* 2010). Our marine dataset does not make easy the differentiation between Eocene formations and Palaeozoic basement on every profile. However, the boundary between these two formations and the Plio-Quaternary units is assumed to correspond to a regional reflector, defined as the top of the undifferentiated substratum and identified on most profiles. The determination of lower units geometry and axial incision depth of palaeovalleys filled by Plio-Quaternary deposits was restricted by the limited penetration of the seismic waves and the presence of a local deaf acoustic facies. Following Thinon *et al.* (2007), we interpret this acoustic mask caused by the presence of biogenic gas in muddy sediments.

### 5.2.3 Palaeovalley network and possible syn-tectonic infilling

According to the seismic data, all the segments of the Machecoul Fault system are southwest dipping normal faults with an apparent subsidence of the hangingwall ( Figs. 5, 7 and 8). It was not possible to determine the accurate dips for all the fault planes (e.g.

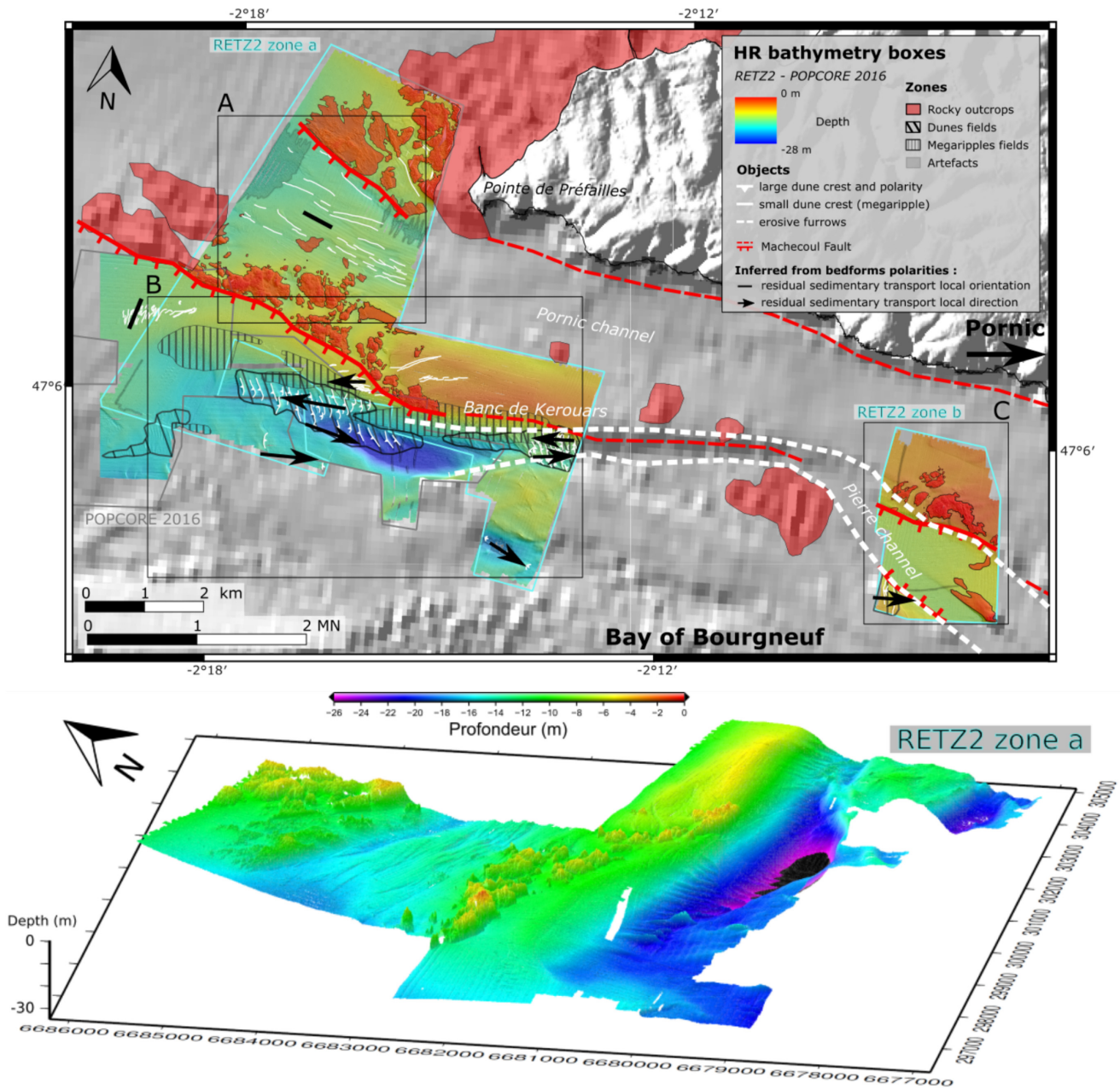


**Figure 7.** Top panel: morphobathymetric map from high resolution bathymetric data acquired during RETZ2 cruise (Kaub *et al.* 2017), merged with POPCORE (Baltzer 2016) data (see text for zones A, B and C descriptions). Frame on Fig. 4. Bottom panel: 3-D view of the main high resolution bathymetric surveyed area (RETZ 2 zone a) using GMT.

on the seismic reflection data because of deaf acoustic facies) but we estimate that the average offshore apparent dip is around  $60^\circ$  to the southwest. On either side of the offshore fault escarpment, the geometry of Us1 top reflector suggests that both walls of the fault are tilted (Fig. 8). On the RETZ2 44 profile (Fig. 8), the hanging-wall bedrock facies (Us2b) probably corresponds to Lutetian and Bartonian limestones.

The palaeovalley network is deeply incised into the Palaeozoic (Us1) and the Eocene (Us2 a and b) basement, reaching up 40 m deep below sea level in the Baie de Bourgneuf (Fig. 8, profile 9 002). The palaeovalley infilling corresponds to the seismic unit U3 and is composed of several incision/filling episodes. Nevertheless, a regional erosive unconformity allows distinguishing two sub-units

U3a and U3b. The U3a unit corresponds to wavy subhorizontal to oblique moderately continuous reflectors and the U3b unit to continuous reflectors with tangential oblique geometry alternating with local slightly transparent-chaotic seismic facies. The diversity of U3a and U3b units facies probably reflects a combination of continental and marine depositional environments. Nonetheless, the tangential-oblique geometry of the U3b unit is quite representative of meander bars or tidal bars which gradually fill preserved valleys during marine flooding stage. Similar facies are well documented in other tidal dominated environments in South Armorican continental shelf (e.g. Traini *et al.* 2013; Gregoire 2016). An uppermost seismic unit U4 is observable on almost all profiles. It seals all the underlying formations by resting on a relative regularly flat

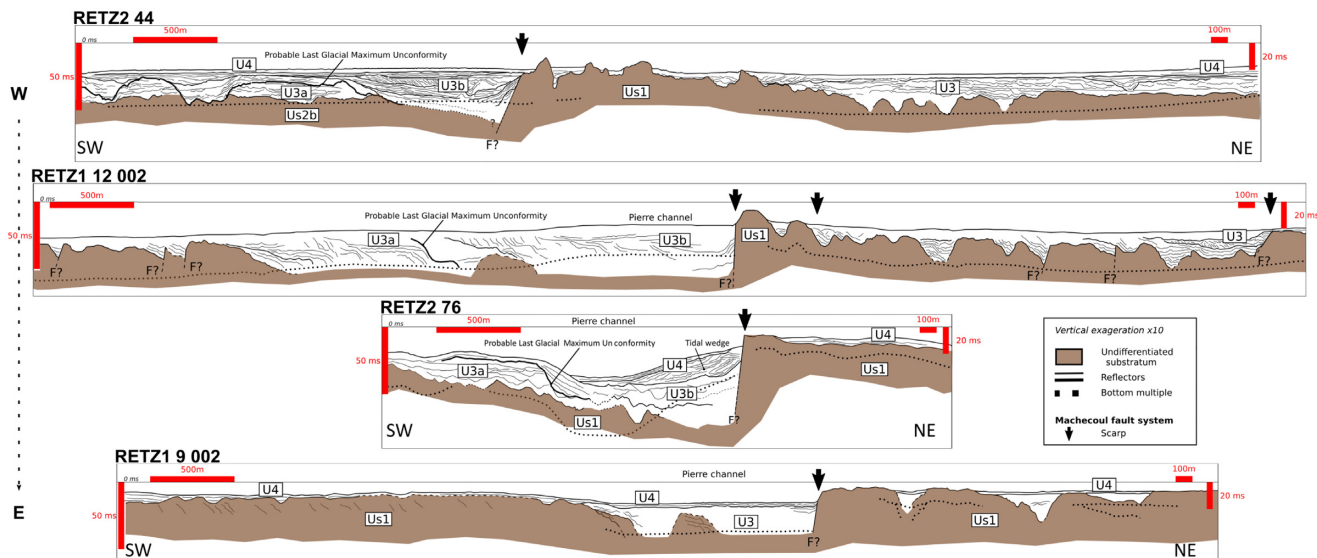


**Figure 8.** Representative sample of interpreted seismic profiles of RETZ1 and 2 cruises (Le Roy *et al.* 2016; Kaub *et al.* 2017), with a 10-times vertical exaggeration (see Fig. 4 for profiles location and appendices Figs. A1 and A2 for raw data, and appendix Fig. A3 for seismic facies description).

surface extending over the palaeovalleys shoulders topography. Its top corresponds to the current seabed. This subhorizontal unit consists of several acoustic facies according to its thickness, ranging from a thin drape whose internal reflectors are masked by the thickness of the bottom signal (Proust *et al.* 2010), to a large thickness of horizontal continuous and subparallel reflectors.

Two mean generations of incisions are preserved in the sedimentary record at the base of the U3a and U3b units. The large amplitude of the erosional unconformity separating the U3a and U3b units is assumed to correspond to the Last Glacial Maximum incision (20 ka) as suggested by Proust *et al.* (2010) for the nearby Loire system and thus interpreted as the result of fluvial incision during sea level drop. These chronostratigraphic attributions suggest that deposits corresponding to the U3a seismic unit are prior to 20 ka and thus that two—or possibly more—Quaternary four order depositional sequences could thus be preserved locally within the Baie de Bourgneuf palaeovalleys network. Anyway, the deposits corresponding to the U3b unit are thus assumed to mostly correspond to Holocene transgressive system track setting during the last sea-level rise. It records some sedimentary structures as channel bars, characteristic of a tidal and/or wave-related dynamics with local ravinement surfaces and or lateral accretion geometries (see Section 5.1 for discussion). Correlatively, the U4 seismic unit is assumed to correspond to the recent and present marine depositional environment with a flat layered sedimentation related to the Holocene sea level stabilization.

The undifferentiated seismic basement appears affected by the Machecoul Fault system (Fig. 7). The top of the undifferentiated unit reaches up locally more than 55 m deep below sea level in the Baie de Bourgneuf. However, to the south-west of the Baie de Bourgneuf, it crops out through the northern part of the Noirmoutier island. The onshore drilling data on the island attests to a thin remnant (less than 5 m) Mesozoic deposits overlaid by about 50 m of Eocene deposits. Further west the top of the undifferentiated seismic basement grades from 40 m deep into the palaeovalley network to 20 or 10 m deep southeastward close to the coastline of the Baie de Bourgneuf (between 10 and 20 m deep). The palaeovalleys incision is large and deeper (up to 55 m deep) in areas where the Machecoul Fault escarpment is well-expressed and the U<sub>s1</sub> basement unit well

constrained by outcrops at the seafloor along the hangingwall of the fault (off Pointe de Préfailles). Our marine dataset thus shows that the Plio-Quaternary sediments are thicker at the bottom of the fault escarpment along the two parallel normal and south-dipping faults of the Machecoul Fault offshore system (Fig. 10). The offshore Plio-Quaternary infilling thickness, deduced from the mapping of the top of the undifferentiated substratum horizon, appears heterogeneous in the Baie de Bourgneuf (Fig. 10). This deposit increases in thickness westward (up to 25 m of Plio-Quaternary sediments in the main valleys). According to these results, the deposition of these units appears to be controlled by the southern escarpment of the Machecoul Fault (Fig. 10 and see Section 5.1 for discussion).

### 5.3 Microseismicity distribution and focal mechanisms

A total of 244 local earthquakes were located along coastal Vendée from 2011 to 2017 using the 3 successive networks described in Section 4.3. Among them, 50 events hypocentres were determined in our area of interest by the VENDE network. In April 2012, a swarm of events was located beneath the Marais Breton basin in the Challans region (Fig. 11a). Most of the hypocentral depths were estimated between 23.5 and 24.8 km. This has to be considered with caution as those events were associated with very large azimuthal gaps (from 270° to 331°, see electronic supplements for catalogue). The 30 events of this swarm occurred within 17 d. All are relatively small, their coda magnitudes ranging from 1.5 to 2.2. Those events are not organized into a main shock–aftershock sequence. Indeed, the largest event of the series occurred on 28 April 2012, in the middle of the series. This swarm, located at the vicinity of the Machecoul Fault, motivated the redeployment of further networks (see Section 4.3). We located 58 local earthquakes between March 2016 and October 2017 from the tighten MACHE network, optimized to get small magnitude signals from the Baie de Bourgneuf/Marais Breton area ( Figs. 4 and 11a).

The mean absolute location errors are  $\pm 4.5$  km in latitude,  $\pm 7.2$  km in longitude and  $\pm 7.6$  km in depth (without outliers on depths). Errors are larger in longitude than in latitude because most of the earthquakes are located outside of the network and/or along an east-west trend (Fig. 11a). Besides, Havskov & Ottemöller (1999)

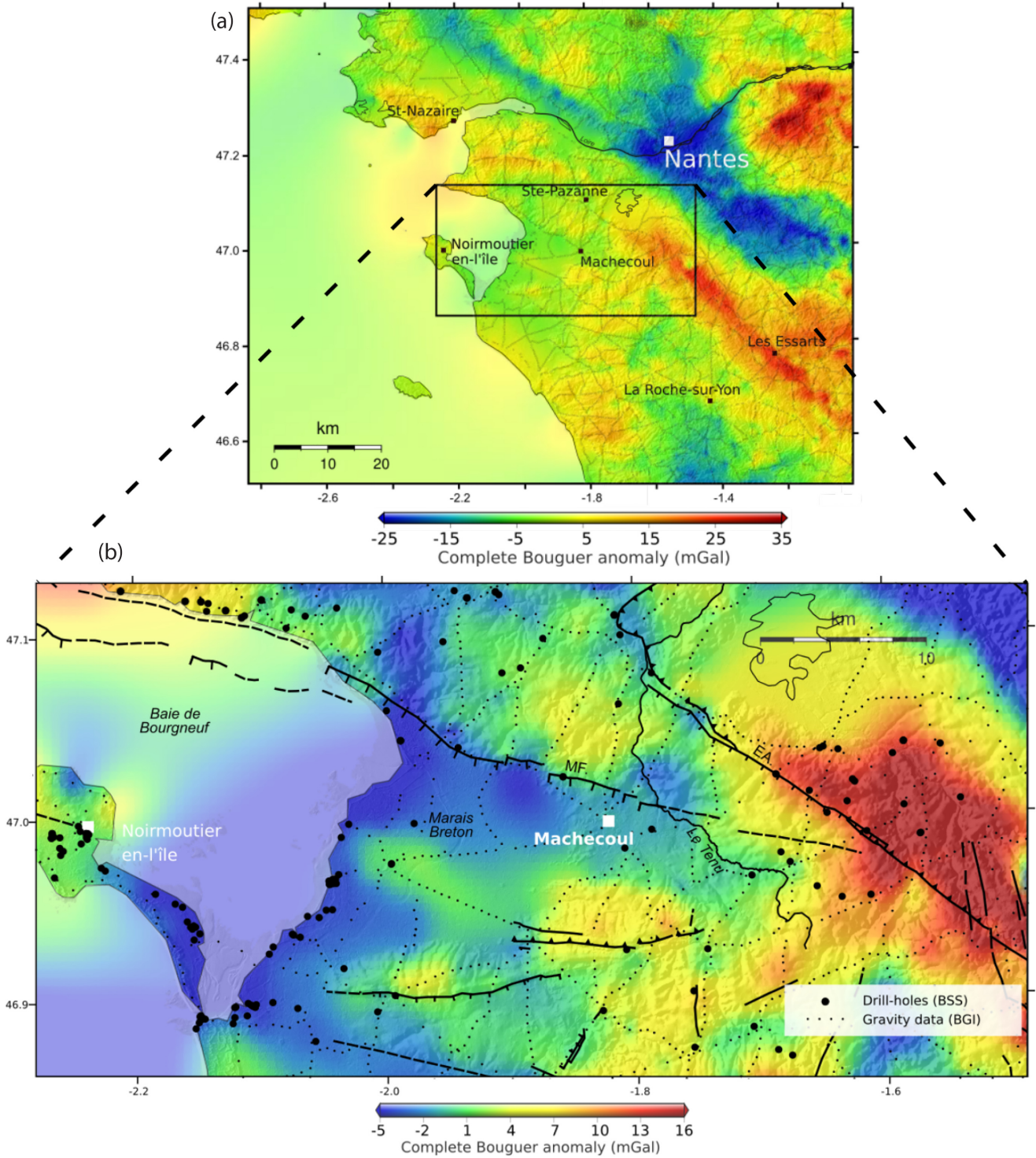


**Figure 9.** (a) Map of complete Bouguer anomaly interpolation calculated from the free air anomaly provided by the BGI around coastal Vendée with an adapted colour-scale and location of the zoomed map. (B) Zoomed map around the Machecoul Fault. A slight white mask is applied to the offshore interpolation, considering the lack of data. Small black circles are gravity data points from BGI, big black circles are drill-holes from BSS used in this study. MF: Machecoul Fault. EA: Les Essarts Accident.

estimated that most stations have to be closer to the epicentre than two times the depth value to get a reliable hypocentral depth, which is not the case for the MACHE network because of its small extent (see electronic supplements for uncertainties). The 58 earthquakes were attributed coda magnitudes between 0.5 and 3.2 and local

magnitude between 0.3 and 3. We estimate the completeness magnitude of the MACHE network probably around  $M_L = 1$ .

Among the 58 earthquakes located, only ten fall within the network. The epicentres distribution is diffuse and widespread. However, the projection of the hypocentres on cross sections normal

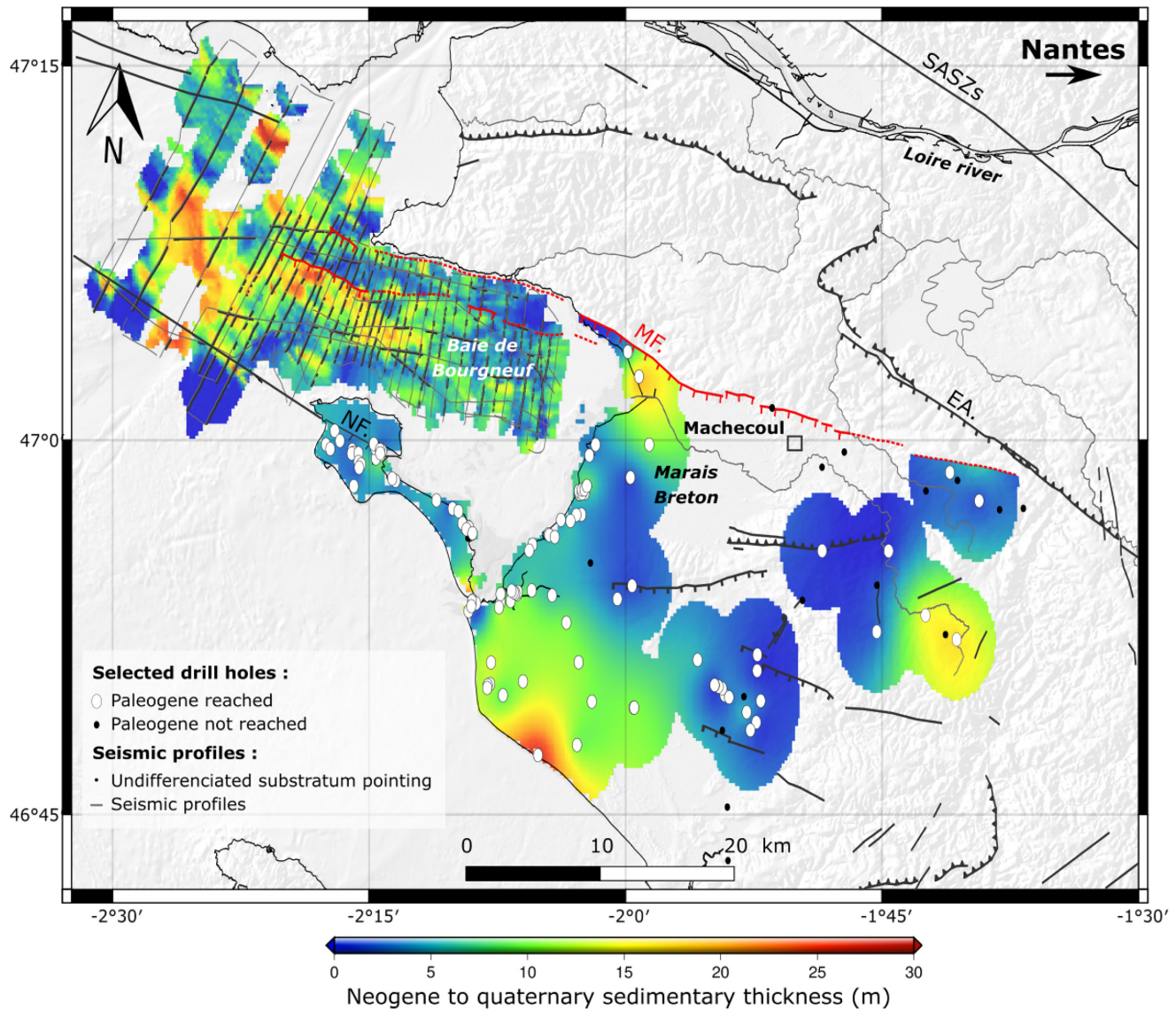


**Figure 10.** Neogene to quaternary sedimentary thickness obtained from onshore drill-holes data (BSS) and seismic profiles from RETZ1 and RETZ2 cruises (Le Roy *et al.* 2016; Kaub *et al.* 2017).

to the fault system show that most of the seismic activity could be located in the vicinity of the Machecoul Fault system (Fig. 11c). The deepest hypocentre fall around 30 km below the surface, revealing an unusually deep seismic activity. The hypocentres depth distribution (Fig. 11c) is bifid: a first maximum between 5 and 15 km depth, and a deeper one at about 20–25 km depth. The focal mechanisms that are determined for the eight events with the smallest azimuthal gap and best polarities fall into two regimes: either strike-slip with plane solution E–W or N–S and a strong dip angle ( $n^{\circ}46$  and  $53$ , Fig. 11b), or a NE–SW extensional regime in the Marais Breton (e.g.  $n^{\circ}23$ , Fig. 11b and electronic supplements for focal solutions). The NE–SW extensional orientation is consistent with the delineation of the Marais Breton and Baie de Bourgneuf basin, south of the WNW–ESE slope break of the Machecoul Fault and associated fault system. Focal solutions in the central zone of the Marais Breton basin could be connected to a microseismic activity on antithetic faults of the Machecoul Fault in the basin. The recorded seismicity at the Machecoul Fault footwall could be connected to

the accident of Les Essarts, a fault supposed to dip southwestward (Fig. 11). We interpret a possible flattening of the fault with depth from the hypocentres distribution. Interpretation of the ‘Armor 2 South’ deep seismic reflection line suggests the existence of subhorizontal shear zones at several depth levels beneath the studied area, the most evident one being at 10–12 km (Bitri *et al.* 2010). Those possible decoupling levels, probably bounding the main thrust units from the inner variscan belt south of the SASZ, are shallower than the depth of our recorded seismicity. However, the same data also image deeper flat-lying levels, notably around 20 km. Admittedly, our seismic database is not enough substantial nor constrained to go further in this interpretation. The stress inversion from the 8 focal solutions results in a dextral–transensional to extensional regime. The  $\sigma_3$  direction is relatively well constrained with a small plunge (N35–N50,  $15^{\circ}$ – $30^{\circ}$ ) and  $\sigma_1$  and  $\sigma_2$  are oblique and distributed along a plane normal to  $\sigma_3$ . This may illustrate a tendency for  $\sigma_1$  and  $\sigma_2$  permutation (see Appendix Fig. C1 for stress inversion).

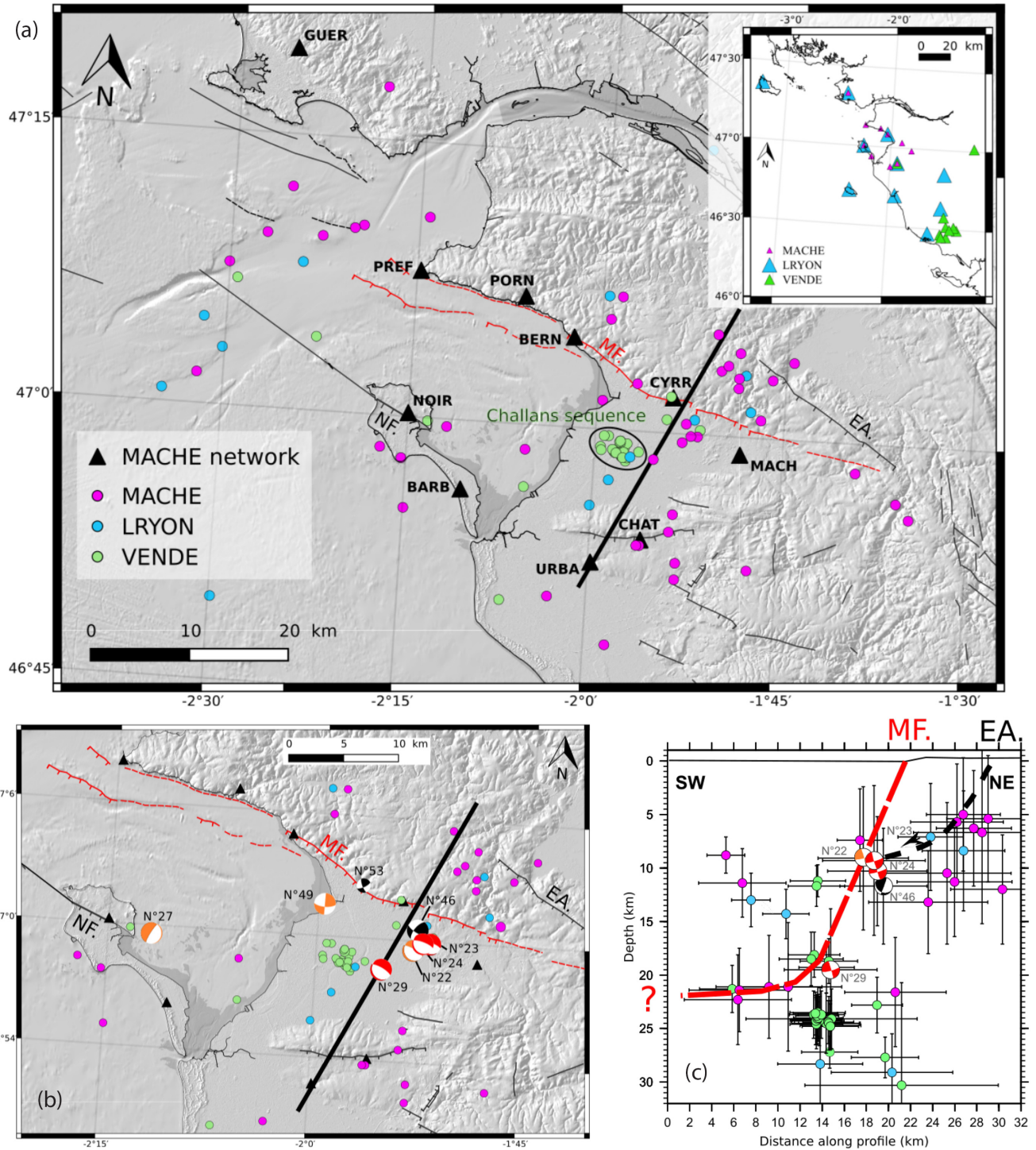


**Figure 11.** (a) Spatial distribution of earthquakes collected between 2011 July and 2017 October in the Marais Breton and Baie de Bourgneuf area (error in depth equal or less than 10 km). Colours represent catalogues of the three different networks (location of stations are represent on the onset map: VENDE network (green), LRYON network (blue) and MACHE network (pink); see electronic supplement for catalogue and uncertainties). MF: Machecoul Fault. NF: Noirmoutier Fault. EA: Les Essarts Accident. (b) Representation of the eight focal mechanisms determined for internal events of the MACHE (2016–2017) network. Colours depending on quality (A black, B orange, C red, see electronic supplement for focal solutions). (c) Cross section normal to the surface expression of the Machecoul Fault. Hypocentres in a 10 km wide area on both sides of the cross-section are projected with error bars (depth and epicentral location, see electronic supplement for catalogue and uncertainties).

## 6 DISCUSSION

### 6.1 Machecoul Fault Neogene activity

We provide evidences of the Plio-Quaternary activity of the Machecoul Fault based on (i) the recent and probably Pliocene incision of the Machecoul Fault footwall relief and (ii) the Plio-Quaternary depocentres distribution onshore and offshore.

The homogeneous relief of the Machecoul Fault footwall might be a Pliocene preserved abrasion surface because of its 45 m altitude in agreement with sea level curve of this geologic time period (Fig. 5d, Barbaroux *et al.* 1983; Haq *et al.* 1987). The low values of incision of the footwall could either indicate a recent incision, supporting the interpretation of a Pliocene preserved palaeosurface (e.g. Telbisz *et al.* 2013), or very low activity rates of the Machecoul Fault (Fig. 6a). However, this abrasion surface is not observed in the hangingwall. Eocene deposits locally preserved in small basins in the footwall (Fig. 3, north of La Bernerie-en-Retz), could indicate an infilling of partly inherited depressions (e.g. Guillocheau *et al.* 2003). Considering the absence of Miocene deposits in coastal Vendée, we interpret the Machecoul Fault Neogene activity from the Plio-Quaternary depocentres distribution. As detailed hereafter, this infilling is not homogeneous and present onshore a maximum thickness of 25 m along the fault, suggesting a link to the Machecoul Fault system (Fig. 10). Offshore, those deposits are preserved in the Machecoul Fault fault controlled palaeovalley system but their potential syntectonic character needs to be examined.

Onshore, the few exploitable drill-holes in the Marais Breton limit the determination of the full basin geometry and infilling. The top of the basement cannot be considered as an isochronous palaeosurface, but provides information on the maximum depth of erosion prior to sedimentary filling, which corresponds to the basin geometry. The Plio-Quaternary deposits distribution is heterogeneously constrained (Fig. 10) but the sediment pile appears to be thicker toward the west both in the Marais Breton and the Baie de Bourgneuf. This could indicate in both cases a westward-increasing syn-tectonic subsidence of the hangingwall along the related Machecoul Fault segments.

In the vicinity of the Machecoul Fault, river incisions in the landscape potentially result from several erosional events of a ‘smooth’ Mio-Pliocene palaeotopography (Brault *et al.* 2004), integrated on the long term, probably since the late Eocene to the early Pleistocene. The strong incision of the main epigenic Tenu river of the area without any perturbation of the longitudinal river profile indicates the antecedence of the Tenu river from the fault escarpment and that erosion rate balance the uplift rate associated with a tectonic activity of the Machecoul Fault (Snyder *et al.* 2000; Montgomery & Brandon 2002).

In the offshore part (Baie de Bourgneuf), thanks to the dense coverage of our seismic reflection data, the palaeovalley system and the Plio-Quaternary thickness are better mapped. In the same way to other studies along the Atlantic coast, the Baie de Bourgneuf bedrock morphology is expected to influence the current sedimentary dynamics of surface formations and the formation of sedimentary patterns at shallow depths, with the effect of local hydrodynamic agents (swell, waves, tide, e.g. Cattaneo & Steel 2003; Chaumillon *et al.* 2008, 2010; Tessier 2012). Even if the palaeovalley morphology of the Baie de Bourgneuf is ancient, both its position and morphology appear to be strongly controlled by the bedrock lithology and tectonics, especially for the Machecoul Fault. The most significant surface erosion at the top of the undifferentiated substratum unit, affected by several faults and most probably

Eocene in age, can be interpreted as the result of the combination of regional tectonic activity and fluvial incision (e.g. Proust *et al.* 2001). The absence of deposits at the footwall which is only constituted by the rocky substratum suggests that the recent deformation is observable only on the hangingwall. The seismic reflectors of the U3a unit show a fan geometry with a thickening close to the fault escarpment. The superficial deposits (e.g. U3b unit) show progradations which could be linked to the tidal banks setting up in the channelized area of the Baie de Bourgneuf due to the scarp orientation (‘rocky-coast valley-fill’ model, Chaumillon *et al.* 2008). This suggest that the deposits were not necessarily initially horizontal and does not guarantee the tectonic origin of the tilting. These tidal structures could be associated with steeply inclined reflectors of limited lateral extension, locally preserved on the hangingwall against the Machecoul Fault scarp (Fig. 8 profiles RETZ2 44, 76 and RETZ1 12 002). The wedge-shaped geometry of the U4 unit and its location in the Pierre Channel lead to interpret this unit as a tidal bar induced by the accentuation of the tidal currents due to the constriction of the channel (Fig. 7). This unit developed by lateral accretion from the fault plane and filled up partially the channel. Consequently, a significant part of the deposits corresponding to U4 unit are against the Machecoul fault scarp and not affected by the fault (Fig. 8 profile RETZ2 76). Locally, when the channel gets wider, the upper part of U4 unit displays extended subhorizontal reflectors sealing the fault (Fig. 8 profile RETZ2 44).

However the deepest reflectors (e.g. U3a unit) showing a low angle dip and a wide lateral extent suggest that there is not solely a tidal origin and could imply a tilting that may have been recorded during the establishment of several sequences (Fig. 8, main palaeovalley on the profile RETZ2 44). The setting up duration of these sequences is not well constrained. Some erosional surfaces (as the latest limiting the superficial unit) could be interpreted as a tidal ravinement surface concomitant with the last transgression without being sequence limits associated with a sea-level fall. Nevertheless, the comparison of these structures from the Baie de Bourgneuf with studies from the Loire estuary suggests that those sequences could be assimilated as fourth order sequences associated with 100 ka glacial-interglacial cycles (Proust *et al.* 2010). The preservation of several depositional sequences is quite rare within palaeovalleys networks previously studied along the Atlantic and Channel proximal continental shelves (Chaumillon *et al.* 2010). It implies a fault motion during several sequences, at least during the last 200 ka, and allowing the preservation of deposits by significant tectonic subsidence. Moreover, other fault controlled Cenozoic shallow basins and channel systems were also imaged by seismic in the Channel as in the Ecrehou basin (Estournes 2011), along the Dover straight (Garcia Moreno 2017), in the Hurd Deep or Western Approaches (Lericolais 1997; Le Roy *et al.* 2011) or Baie of Concarneau in South Brittany (Menier 2004). Nevertheless, evidence of Quaternary tectonics remains difficult for all these systems and potential fault offsets remain mostly below the metric resolution of the single-channel seismic-reflection data. The syn-tectonic potential of the tilted sedimentary record against the Machecoul Fault is limited by the resolution of our seismic reflection data.

Numerous previous studies along the inner continental shelves of French Atlantic and Channel have shown that preservation of sediment bodies in palaeovalley fills are mainly controlled by tidal hydrodynamics amplified by local constrictions of the incised valleys (Chaumillon *et al.* 2010). Thus, despite the combination of several complementary data and methods, none of the approaches definitively attests or discriminates the tectonic origin of the Plio-Quaternary infilling of the Marais Breton and Baie de Bourgneuf.

## 6.2 Machecoul Fault present-day activity

Since 2011, the earthquakes located in the vicinity of the Machecoul Fault show no spatio-temporal organizations, except for the Challans swarm (2012). The Marais Breton seismicity is then conform to the diffuse Massif Armorican seismicity. However, the event depth ranging from 5 to 30 km were unexpected in this area. In the Armorican Massif, lithological crustal heterogeneities inducing rheological anisotropy may affect seismicity distribution (Mazabraud 2004; Arroucau 2006). In the Marais Breton, most of the events are located in between 12 and 15 km, that is within the expected seismogenic upper crust (Mazabraud *et al.* 2005; Perrot *et al.* 2005) but part of the 2012 Challans swarm and of our new recorded additional events are on average as deep as  $24.2 \pm 2.3$  km deep and  $26.3 \pm 7.2$  km deep, respectively. The maximum depth of earthquakes has long been used to constrain the seismogenic thickness of the upper part of the lithosphere (e.g. Meissner & Strehlau 1982). It is a good indicator of the brittle–ductile transition which may, in turn, give insight into the geothermal gradient in the crust (e.g. Sibson 1982; Lamontagne & Ranalli 1996; Albaric 2009). The seismogenic thickness can reciprocally be roughly estimated from the geotherm (e.g. Vigneresse *et al.* 1988). Considering the low surface heat flow measured in coastal Vendée ( $<50$  mW m<sup>-2</sup>, Jolivet *et al.* 1989) and a crust thickness around 30 km (e.g. Grad *et al.* 2009), a temperature of 300 °C could be reached between 15 and 25 km depth (Vigneresse *et al.* 1988), the upper bound of quartz dislocation creep (e.g. Sibson 1982). Such temperature is consistent with a brittle lower crust and thus with the around 25 km focal depths obtained in our study. The coastal Vendée seismogenic crust appears to be thicker than in the whole Armorican Massif, at least locally in the Marais Breton. Our focal solutions being not well-constrained partly because of the poor azimuthal coverage of the stations in the Armorican Massif, the extensional and strike-slip solutions are usually equiprobable. Furthermore, while nodal directions are compatibles, our events have small magnitudes, so are therefore difficult to link with surface trends and major crustal faults as the Machecoul Fault or the Les Essarts accident. Neotectonic structures have been described in western Vendée and associated with a quaternary extensive tectonic activity of the Machecoul Fault (Baize *et al.* 2002). Among them, we measured a set of small-scale tension–shear joints and dip-slip normal faults (see Fig. 3 and Appendix Fig. D1) which were previously described by Baize *et al.* (2002). Those syn- or post-sedimentary small structures affect units of pebbles of unconstrained Pliocene to Quaternary age at the footwall of the MF, along the cliffs NW of La Bernerie-en-Retz (Figs. 3 and D1). Those minor faults, parallel to the offshore Machecoul Fault, are mechanically compatible with the overall trend of  $\sigma_3$  given by the inversion of the focal mechanism (see Appendix Fig. C1). Although we only could extract eight focal solutions, the minimum subhorizontal stress we computed ( $\sigma_3$  striking  $\sim$ N30–N45, Fig. C1) is in good agreement with previous regional study (Nicolas *et al.* 1990; Mazabraud *et al.* 2005).

## 6.3 Could the Machecoul Fault system generate the Bouin 1799 event?

Limasset *et al.* (1992) proposed that the 1799 seismic rupture would be associated with an assumed extension to the east of the Noirmoutier fault, which is located west of the Marais Breton/Baie de Bourgneuf basin. This extension of the fault seems unlikely given the surface and subsurface geology of the area. Moreover, the Noirmoutier Fault is dipping southwest. An hypocentre on this fault, at

the brittle–ductile transition would lead to an epicentre significantly south of the Noirmoutier Fault trace (i.e. much farther the epicentre area as determined by Baumont & Scotti 2011). This is unlikely given the absence of accounts of high macroseismic intensities further kilometers south of the Noirmoutier Fault. We therefore favour instead a scenario involving the rupture of the Machecoul Fault. Indeed, this scenario would be consistent with the occurrence of a precursor felt only at Machecoul, in the vicinity of the eponymous fault a few hours before the main shock. In addition, several geological indices, including neotectonic structures (Baize *et al.* 2002) and the thicker Plio-Quaternary deposits at the toe of its escarpment, as well as the presence of a mid-crustal seismicity suggest that the Machecoul Fault could be active. All of these arguments lead us to propose the Machecoul Fault to be at the origin of the 1799 Vendée earthquake. The magnitude previously associated with the 1799 earthquake from  $M_w$  5.41 to 6.64 are values compatible with rupture of fault segments of about 5–15 km length. Our work shows that some of the Machecoul Fault segments lengths (which range from 2 to 15 km length) are consistent with the occurrence of a magnitude 6 earthquake. As discussed earlier, a brittle–ductile transition at depths around 20–25 km in the fault vicinity is possible. Such depth is both consistent with those of the microseismicity and of the 1799 macroseismic field (Baumont & Scotti 2011). An earthquake nucleating at  $\sim$ 20–25 km on a 60° dipping normal fault and breaking the surface would rupture a very large fault surface (given the aspect ratio of a rupture zone in Wells & Coppersmith 1994). Only the scenarios associated with the largest magnitude for the event are likely to propagate a rupture up to the surface. The probability that the 1799 earthquake ruptured the surface along one of the fault segments of the Marais Breton is therefore low. However the existence, both onshore and offshore, of a decametric-scale scarp and the possibility that the Machecoul Fault was active since several million years could indicate that past earthquakes of larger magnitudes or shallower depths occurred in the past probably with very large inter-seismic periods.

Indeed, assuming that the sediment deposition along the fault exactly compensates the depositional space created by the fault activity during the Plio-Quaternary, we obtain a cumulative vertical displacement between 20 and 25 m (for onshore and offshore estimates respectively). This yields a vertical slip rate between 0.005 and 0.01 mm yr<sup>-1</sup>, depending on the age of the base of the Pliocene considered (5–2.5Ma). Considering a fault dip around 60°, the extension and slip rates fall in similar value ranges.  $M5+$  (or  $M6+$ ) earthquakes accommodating 10 cm (or 1 m) of coseismic slip on a given Machecoul fault segment may then have a recurrence of 10 000 (or 100 000) yr. These results are based on the initial hypothesis, rather conservative given the significant transgressions and regressions that happened in the region since the Pliocene. However, the values we obtain are roughly compatible with the present N–S extension rates for eastern Brittany estimated after two decades of geodetic measurements at  $0.3$ – $0.7 \times 10^{-9}$  yr<sup>-1</sup>, a value still associated with relatively high uncertainties, requiring that the slip on the fault do not exceed 0.1 mm yr<sup>-1</sup> (Masson *et al.* 2019).

The seismogenic potential of the faults in metropolitan France is still associated to very large epistemic uncertainties. In most SHA study, the instrumental and historical seismicity remains associated to large seismotectonic zones (e.g. Marin *et al.* 2004; Drouet *et al.* 2020) where the individual faults are rarely taken into account. It is particularly true along the western coast of France, where the active fault potential is difficult to evaluate (e.g. Baize *et al.* 2013; Jomard *et al.* 2017). Despite remaining uncertainties about an elusive surface rupture on the Machecoul Fault, following some early

propositions by Baize *et al.* (2013) and Jomard *et al.* (2017), our study documents new arguments suggesting that this fault is a likely source for the 1799 earthquake, but it still lacks direct offset measurements and a potential to estimate accurate slip rates. Further studies, involving subsurface geophysics, neotectonics and palaeoseismological surveys are required in order to eventually demonstrate the relation between the fault and earthquake, as well as to quantify the rate of slip along the fault and the return period of the surface rupturing.

## 7 CONCLUSION

This study is a first tentative effort to document the geology and the geomorphology in the vicinity of the epicentre of the 1799 damaging historical Vendée earthquake in western France with a pluridisciplinary approach in order to better estimate the seismic hazard in this region. We provided various data set of marine geophysics (40 km<sup>2</sup> of high-resolution bathymetry data and more than 700 km of seismic reflection profiles acquired simultaneously with single-channel streamer and sub-bottom profiler) and seismology (temporary microseismicity experiment) jointly analyzed with pre-existing data to benefit from a better knowledge of the coastal Vendée geology and tectonic activity.

We tried to highlight the fault activity on a broad timescale coupling historical and instrumental seismicity with geological setting and long term evolution (studying basins with drilling, seismic, gravity and morphotectonics). Holocene activity along the Machecoul Fault trace can not be firmly demonstrated but the new data obtained in the framework of this study are far from being contradictory with this interpretation, all the more so as we have highlighted a seismic activity of the Machecoul Fault at depth. To better understand the local seismicity, there is a need for larger events than those recorded these last few years, with better constrained focal solutions and magnitudes compatible with not only fracturation but fault surface rupture. Thus, given the low seismicity rates, we have continued to monitor the local seismicity with our dedicated seismological network. Besides, further investigations should be carried out in the vicinity of the Machecoul Fault like offshore infilling dating to constrains the age of the deposits and better estimate the deformation rates, and near-surface onshore geophysical survey to better constrain the fault and basin geometry as well as the sediment thickness.

## ACKNOWLEDGEMENTS

We thank Stéphane Baize and an anonymous reviewer for their very constructive suggestions that strongly improved the paper. This study represents part of the PhD project of the first author. This work, supported by the Conseil Départemental de la Vendée (CDV), is a joint project which benefited from an Université de Bretagne Occidentale (UBO) doctoral grant and CEA financial support. We are grateful for the technical assistance of Jean-Pierre Laurent (CDV, seismic installations and servicing) and Christophe Prunier (UBO, seismic installations and servicing and seismic/bathymetry). We greatly thank the RV Haliotis crew (IFREMER and GENAVIR) for both cruises within this project. We acknowledge Agnès Baltzer (IGARUN) for sharing the POPCORE 2016 high-resolution bathymetric data. We also want to thank Christel Tiberi and Matthieu Plasman (Géosciences Montpellier) for their expertise with gravity processing and interpretation.

## REFERENCES

- Ahnert, F., 1984. Local relief and the height limits of mountain ranges, *Am. J. Sci.*, **284**(9), 1035–1055.
- Albaric, J., 2009. Relationship between active deformation, rheology and magmatism in a continental rift context: seismological study of the North Tanzanian Divergence, East African Rift, *Theses*, Université de Bretagne Occidentale - Brest.
- Allen, R.V., 1978. Automatic earthquake recognition and timing from single traces, *Bull. seism. Soc. Am.*, **68**(5), 1521–1532.
- Arroucau, P., 2006. Seismicity of the Armorican Massif: relocations and tectonic interpretation, *Theses*, Université de Nantes.
- Audin, L., Avouac, J.-P., Flouzat, M. & Plantet, J.-L., 2002. Fluid-driven seismicity in a stable tectonic context: the Remiremont fault zone, Vosges, France, *Geophys. Res. Lett.*, **29**(6), 13–1.
- Baize, S., Cushing, M., Lemeille, F., Granier, T., Grellet, B., Carbon, D., Combes, P. & Hibs, C., 2002. *Inventaire des indices de rupture affectant le Quaternaire, en relation avec les grandes structures connues, en France métropolitaine et dans les régions limitrophes*, Vol. **175**, Mémoires de la Société Géologique de France.
- Baize, S., Cushing, E.M., Lemeille, F. & Jomard, H., 2013. Updated seismotectonic zoning scheme of Metropolitan France, with reference to geologic and seismotectonic data, *Bull. Soc. Géol. Fr.*, **184**(3), 225–259.
- Ballèvre, M., Bosse, V., Ducassou, C. & Pitra, P., 2009. Palaeozoic history of the Armorican Massif: models for the tectonic evolution of the suture zones, *Compt. Rend. Geosci.*, **341**(2–3), 174–201.
- Baltzer, A., 2016. POPCORE cruise, RV Haliotis, doi:10.17600/16005300.
- Barbaroux, L., Cavet, P., *et al.*, 1983. Notice explicative de la carte géologique de France 1/50 000, feuille de Nort-sur-Erdre (1222), BRGM, Orléans, 48p.
- Barrois, C., 1921. Rapport sur les feuilles de Dinan et de Saint-Nazaire à 1/80 000, *Bull. Soc. Géol. Fr.*, **26**, 45–48.
- Baumont, D. & Scotti, O., 2011. The French Parametric Earthquake Catalogue (FPEC) based on the best events of the SisFrance macroseismic database-version 1.1, Tech. rep., IRSN/DEI/2011-012.
- Béchenec, F., 2007. Carte géologique harmonisée du département de Loire-Atlantique, BRGM, Orléans, 369.
- Béchenec, F., 2009. Carte géologique harmonisée du département de la Vendée, BRGM, Orléans, 348.
- Bessin, P., Guillocheau, F., Robin, C., Schroëtter, J.-M. & Bauer, H., 2015. Planation surfaces of the Armorican Massif (western France): denudation chronology of a Mesozoic land surface twice exhumed in response to relative crustal movements between Iberia and Eurasia, *Geomorphology*, **233**, 75–91.
- Bilham, R., 2004. Urban earthquake fatalities: a safer world, or worse to come? *Seismol. Res. Lett.*, **75**(6), 706–712.
- Bitri, A., Brun, J.-P., Gapais, D., Cagnard, F., Gumiaux, C., Chantraine, J., Martelet, G. & Truffert, C., 2010. Deep reflection seismic imaging of the internal zone of the South Armorican Hercynian belt (western France)(ARMOR 2/Géofrance 3D Program), *Comp. Rend. Geosci.*, **342**(6), 448–452.
- Blakely, R.J., 1995. *Potential Theory in Gravity and Magnetics*, Cambridge Univ. Press.
- Bonnet, S., Guillocheau, F., Brun, J.-P. & Van Den Driessche, J., 2000. Large-scale relief development related to Quaternary tectonic uplift of a Proterozoic-Paleozoic basement: the Armorican Massif, NW France, *J. geophys. Res.*, **105**(B8), 19 273–19 288.
- Borne, V., 1986. Le Paléogène du bassin de Challans-Noirmoutier (France), *PhD thesis*, Thèse de l'Université de Nantes.
- Borne, V., Chevalier, M. & Olivier-Pierre, M., 1989. Les premiers dépôts paléogènes (yprésiens) de la bordure méridionale du Massif armoricain; aspects sédimentologique, tectonique et paléogéographique, *Géologie de la France*, **1–2**, 11–20.
- Borne, V., Margerel, J.-P. & Olivier-Pierre, M., 1991. L'évolution des paléoenvironnements au Paléogène dans l'Ouest de la France; le bassin de Saffre-Nord-sur-Erdre (Loire-Atlantique, France), *Bull. Soc. Géol. Fr.*, **162**(4), 739–751.
- Brault, N., Guillocheau, F., Proust, J.-N., Nalpas, T., Brun, J.-P., Bonnet, S. & Bourquin, S., 2001. Le système fluvio-estuarien Pléistocène

- moyen-supérieur de Pénestin (Morbihan); une paléo-Loire ? *Bull. Soc. Géol. Fr.*, **172**(5), 563–572.
- Brault, N., *et al.*, 2004. Mio–Pliocene to Pleistocene palaeotopographic evolution of Brittany (France) from a sequence stratigraphic analysis: relative influence of tectonics and climate, *Sediment. Geol.*, **163**(3–4), 175–210.
- Brocklehurst, S.H. & Whipple, K.X., 2002. Glacial erosion and relief production in the Eastern Sierra Nevada, California, *Geomorphology*, **42**(1–2), 1–24.
- Bullard, T.F. & Lettis, W.R., 1993. Quaternary fold deformation associated with blind thrust faulting, Los Angeles Basin, California, *J. geophys. Res.*, **98**(B5), 8349–8369.
- Burbank, D.W. & Anderson, R.S., 2011. *Tectonic Geomorphology*. John Wiley & Sons.
- Calais, E., Camelbeeck, T., Stein, S., Liu, M. & Craig, T., 2016. A new paradigm for large earthquakes in stable continental plate interiors, *Geophys. Res. Lett.*, **43**(20), doi:10.1002/2016GL070815.
- Cara, M., *et al.*, 2015. SI-Hex: a new catalogue of instrumental seismicity for metropolitan France, *Bull. Soc. Géol. Fr.*, **186**(1), 3–19.
- Casey, R. & DMC, I., 2012. Portable Data Collection Center (PDCC) v3. 8 User Manual, Incorporated Research Institutions for Seismology (IRIS), Washington, DC.
- Cattaneo, A. & Steel, R.J., 2003. Transgressive deposits: a review of their variability, *Earth-Sci. Rev.*, **62**(3–4), 187–228.
- Chaumillon, E., Proust, J.-N., Menier, D. & Weber, N., 2008. Incised-valley morphologies and sedimentary-fills within the inner shelf of the bay of Biscay (France): a synthesis, *J. Mar. Syst.*, **72**(1–4), 383–396.
- Chaumillon, E., Tessier, B. & Reynaud, J.-Y., 2010. Stratigraphic records and variability of incised valleys and estuaries along french coasts, *Bull. Soc. Géol. Fr.*, **181**(2), 75–85.
- Craig, T., Calais, E., Fleitout, L., Bollinger, L. & Scotti, O., 2016. Evidence for the release of long-term tectonic strain stored in continental interiors through intraplate earthquakes, *Geophys. Res. Lett.*, **43**(13), 6826–6836.
- Delanoë, Y., 1988. Les grands traits de la structure et de l'évolution géodynamique des dépôts tertiaires du plateau continental sud-armoricain d'après les enregistrements de réflexion sismique, *Géologie de la France*, **1**, 79–90.
- Delanoë, Y., Margerel, J. & Pinot, J., 1976. En Baie de Concarneau, l'Oligocène marin est discordant sur un Eocène ondulé, faillé et érodé, et l'Aquitainien a voilé l'ensemble après une nouvelle pénéplation, *CR Acad. Sci. Paris*, **282**, 29–32.
- Drouet, S., Ameri, G., Le Dortz, K., Secanell, R. & Senfaute, G., 2020. A probabilistic seismic hazard map for the metropolitan France, *Bulletin of Earthquake Engineering*, **18**(5), 1865–1898.
- Durand, S., 1960. *Le Tertiaire de Bretagne: étude stratigraphique, sédimentologique et tectonique*, **12**, Mém. Soc. géol. minér. Bretagne.
- Duverger, C., Mazet-Roux, G., Bollinger, L., Guilhem Trilla, A., Vallage, A., Hernandez, B. & Cansi, Y., submitted. A decade of seismicity in metropolitan France (2010-2019): the CEA/LDG methodologies and observations, *Bull. Soc. Géol. Fr.*
- Dyer, K.R. & Huntley, D.A., 1999. The origin, classification and modelling of sand banks and ridges, *Continent. Shelf Res.*, **19**(10), 1285–1330.
- Ellsworth, W.L., Llenos, A.L., McGarr, A.F., Michael, A.J., Rubinstein, J.L., Mueller, C.S., Petersen, M.D. & Calais, E., 2015. Increasing seismicity in the US midcontinent: Implications for earthquake hazard, *Leading Edge*, **34**(6), 618–626.
- Estournes, G., 2011. Architectures et facteurs de contrôle des bassins quaternaires immergés du précontinent armoricain: exemples de la paléovallée d'Étel (Bretagne Sud) et du bassin des Ecrehou (Golfe normand Breton), *PhD thesis*, Université de Bretagne Sud.
- Fäh, D., Kind, F., Lang, K. & Giardini, D., 2001. Earthquake scenarios for the City of Basel, *Soil Dyn. Earthq. Eng.*, **21**(5), 405–413.
- García Moreno, D., 2017. Origin and geomorphology of the Dover Strait and southern North Sea palaeovalleys and palaeo-depressions, *PhD thesis*, Ghent University.
- García-Moreno, D., *et al.*, 2015. Fault activity in the epicentral area of the 1580 Dover Strait (Pas-de-Calais) earthquake (northwestern Europe), *J. geophys. Int.*, **201**(2), 528–542.
- Gautier, M., 1962. La dépression de Toulven et l'évolution morphologique de la Bretagne sud-occidentale depuis le début de l'éocène, *Norvès*, **35**(1), 265–290.
- Gautier, M., 1969. Les sablières des environs de Pornic (L.-A.) et le Pliocène du pays de Retz, *Norvès*, **62**(1), 155–176.
- Gebelin, A., Martelet, G., Brunel, M., Faure, M. & Rossi, P., 2004. Late hercynian leucogranites modelling as deduced from new gravity data: the example of the millevaches massif (massif central, France), *Bull. Soc. Géol. Fr.*, **175**(3), 239–248.
- Gouleau, D., 1968. Etude hydrologique et sédimentologique de la baie de Bourgneuf, *PhD thesis*, Université de Caen.
- Grad, M., Tiira, T. & Group, E.W., 2009. The moho depth map of the european plate, *J. geophys. Int.*, **176**(1), 279–292.
- Gregoire, G., 2016. Dynamique sédimentaire et évolution holocène d'un système macrotidal semi-fermé: l'exemple de la rade de Brest, *PhD thesis*, Université de Bretagne Occidentale, Brest.
- Guillocheau, F., Brault, N., Thomas, E., Barbarand, J., *et al.*, 2003. Histoire Géologique du Massif Armoricaïn depuis 140 Ma (Crtac-Actuel), *Bulletin d'Information des Géologues du Bassin de Paris*, **40**(1), 13–28.
- Hanks, T.C. & Johnston, A.C., 1992. Common features of the excitation and propagation of strong ground motion for North American earthquakes, *Bull. seism. Soc. Am.*, **82**(1), 1–23.
- Haq, B.U., Hardenbol, J. & Vail, P.R., 1987. Chronology of fluctuating sea levels since the Triassic, *Science*, **235**(4793), 1156–1167.
- Haugmard, M., 2016. Détermination non-linéaire des paramètres hypocentraux et structuraux: application à la sismicité intracontinentale du Massif armoricaïn, *PhD thesis*, Université Bretagne Loire.
- Havskov, J. & Ottemöller, L., 1999. SEISAN earthquake analysis software, *Seismol. Res. Lett.*, **70**(5), 532–534.
- Huerta, P., Proust, J.-N., Guennoc, P. & Thinon, I., 2010. Seismic stratigraphy of the Vendean-Armorican platform of the French Atlantic shelf: new insights into the history of the North Atlantic ocean, *Bull. Soc. Géol. Fr.*, **181**(1), 37–50.
- Hutton, L. & Boore, D.M., 1987. The ML scale in southern California, *Bull. seism. Soc. Am.*, **77**(6), 2074–2094.
- Jaeger, J.-L., 1967. Un alignement d'anomalies légères coïncidant avec des bassins tertiaires en Bretagne, *Mém. BRGM*, **52**, 91–102.
- Jaeger, J.-L. & Corpel, J., 1967. étude de l'anomalie gravimétrique légère en relation avec le bassin tertiaire de Rennes, *Mém. BRGM*, **52**, 103–129.
- Johnston, A.C., 1989. The seismicity of stable continental interiors, in *Earthquakes at North-Atlantic Passive Margins: Neotectonics and Postglacial Rebound*, pp. 299–327, Springer.
- Jolivet, J., Bienfait, G., Vignerresse, J. & Cuney, M., 1989. Heat flow and heat production in Brittany (Western France), *Tectonophysics*, **159**(1–2), 61–72.
- Jomard, H., Cushing, E.M., Palumbo, L., Baize, S., David, C. & Chartier, T., 2017. Transposing an active fault database into a seismic hazard fault model for nuclear facilities—Part 1: building a database of potentially active faults (B DFA) for metropolitan France, *Nat. Haz. Earth Syst. Sci.*, **17**(9), 1573–1584.
- Kaub, C., Le Roy, P. & Geoffroy, L., 2017. RETZ2 cruise, RV Haliotis, doi:10.17600/17008300.
- Lamontagne, M. & Ranalli, G., 1996. Thermal and rheological constraints on the earthquake depth distribution in the Charlevoix, Canada, intraplate seismic zone, *Tectonophysics*, **257**(1), 55–69.
- Le Roy, P., *et al.*, 2011. Cenozoic tectonics of the Western Approaches Channel basins and its control of local drainage systems, *Bull. Soc. Géol. Fr.*, **182**(5), 451–463.
- Le Roy, P., Kaub, C. & Geoffroy, L., 2016. RETZ1 cruise, RV Haliotis, doi:10.17600/16013000.
- Lee, W.H.K., Bennett, R. & Meagher, K., 1972. A method of estimating magnitude of local earthquakes from signal duration, US Department of the Interior, Geological Survey.
- Lericolais, G., 1997. Évolution Plio-quaternaire du Fleuve Manche: stratigraphie et Géomorphologie d'une plateforme continentale en régime périglaciaire, *PhD thesis*, Bordeaux 1.

- Lesueur, P. & Klingébiel, A., 1986. Carte et notice de répartition des sédiments superficiels du plateau continental du Golfe de Gascogne, partie septentrionale (éch.: 1/500 000), *Coédition BRGM/IFREMER Carte géologique de la marge continentale française*, **1**.
- Lienert, B.R., Berg, E. & Frazer, L.N., 1986. HYPOCENTER: An earthquake location method using centered, scaled, and adaptively damped least squares, *Bull. seism. Soc. Am.*, **76**(3), 771–783.
- Limasset, J.-C., Limasset, O. & Martin, J.-C., 1992. Histoire et étude des séismes, in *Annales de Bretagne et des pays de l'Ouest*, pp. 97–116, Persée-Portail des revues scientifiques en SHS.
- Manchuel, K., Traversa, P., Baumont, D., Cara, M., Nayman, E. & Durouchoux, C., 2017. The French seismic CATalogue (FCAT-17), *Bull. Earthq. Eng.*, **162**, 227–2251.
- Marin, S., Avouac, J.-P., Nicolas, M. & Schlupp, A., 2004. A probabilistic approach to seismic hazard in metropolitan France, *Bull. seism. Soc. Am.*, **94**(6), 2137–2163.
- Masson, C., Mazzotti, S., Vernant, P. & Doerflinger, E., 2019. Extracting small deformation beyond individual station precision from dense Global Navigation Satellite System (GNSS) networks in France and western Europe, *Solid Earth*, **10**(6), 1905–1920.
- Mazabraud, Y., 2004. Déformation active d'une région intraplaque à déformation lente: le cas de la France: sismicité et modélisations thermomécaniques 2D et 3D, *PhD thesis*, Université de Nice.
- Mazabraud, Y., Béthoux, N., Guilbert, J. & Bellier, O., 2005. Evidence for short-scale stress field variations within intraplate central-western France, *J. geophys. Int.*, **160**(1), 161–178.
- Mazabraud, Y., Béthoux, N. & Delouis, B., 2013. Is earthquake activity along the French Atlantic margin favoured by local rheological contrasts? *Compt. Rend. Geosci.*, **345**(9–10), 373–382.
- Mazzotti, S. *et al.*, submitted. FMHex20: a database of earthquake focal mechanisms in metropolitan France and conterminous Western Europe, *BSGF - Earth Sci. Bull.*, doi:10.1051/bsgf/2020049.
- Medvedev, S., Sponheuer, W. & Kárník, V., 1967. Seismic intensity scale, version 1964 (MSK-64), *Inst. Geodyn., Jena, Germany, Publ.*, **48**, 13.
- Meissner, R. & Strehlau, J., 1982. Limits of stresses in continental crusts and their relation to the depth-frequency distribution of shallow earthquakes, *Tectonics*, **1**(1), 73–89.
- Menier, D., 2004. Morphologie et remplissage des vallées fossiles sud-armoricaines : apport de la stratigraphie sismique, *PhD thesis*, Université de Rennes 1.
- Menier, D., Reynaud, J., Proust, J.-N., Guillocheau, F., Guennoc, P., Tessier, B., Bonnet, S. & Goubert, E., 2006a. Inherited fault control on the drainage pattern and infilling sequences of late glacial incised valley, SE coast of Brittany, France, *Spec. Publ. SEPM*, **85**, 85–98.
- Menier, D., Reynaud, J.-Y., Proust, J.-N., Guillocheau, F., Guennoc, P., Bonnet, S., Tessier, B. & Goubert, E., 2006b. Basement control on shaping and infilling of valleys incised at the southern coast of Brittany, France, *Spec. Publ. SEPM*, **85**, 37–55.
- Menier, D., Augris, C. & Briand, C., 2014. *Les réseaux fluviaux anciens du plateau continental de Bretagne Sud*, Atlas & cartes, Ed. Quae.
- Mitchum, R., Jr, Vail, P. & Thompson, S., III, 1977. Seismic stratigraphy and global changes of sea level: Part 2. the depositional sequence as a basic unit for stratigraphic analysis: Section 2. application of seismic reflection configuration to stratigraphic interpretation, in *AAPG MEMOIR Seismic Stratigraphy — Applications to Hydrocarbon Exploration*, Vol. **26**, pp. 53–62, American Association of Petroleum Geologists.
- Montgomery, D.R. & Brandon, M.T., 2002. Topographic controls on erosion rates in tectonically active mountain ranges, *Earth planet. Sci. Lett.*, **201**(3–4), 481–489.
- Nicolas, M., Santoiro, J. & Delpech, P., 1990. Intraplate seismicity: new seismotectonic data in western Europe, *Tectonophysics*, **179**(1), 27–53.
- Nocquet, J.-M., 2012. Present-day kinematics of the mediterranean: a comprehensive overview of GPS results, *Tectonophysics*, **579**, 220–242.
- Peckham, S., 2003. RiverTools Users Guide, Rivix, LLC, Boulder, CO.
- Perrot, J. *et al.*, 2005. Analysis of the Mw 4.3 Lorient earthquake sequence: a multidisciplinary approach to the geodynamics of the Armorican Massif, westernmost France, *J. geophys. Int.*, **162**(3), 935–950.
- Petersen, M.D., *et al.*, 2015. The 2014 United States national seismic hazard model, *Earthq. Spectra*, **31**(S1), S1–S30.
- Proust, J.-N., Menier, D., Guillocheau, F., Guennoc, P., Bonnet, S., Rouby, D. & Le Corre, C., 2001. Fossil valleys in the Bay of Vilaine (Brittany, France): nature and evolution of the pleistocene coastal sediment wedge of brittany [Les vallées fossiles de la Baie de la Vilaine: nature et évolution du prisme sédimentaire côtier du pleistocène armoricain], *Bull. Soc. Géol. Fr.*, **172**(6), 737–749.
- Proust, J.-N., Renault, M., Guennoc, P. & Thion, I., 2010. Sedimentary architecture of the Loire River drowned valleys of the French Atlantic shelf, *Bull. Soc. Géol. Fr.*, **181**(2), 129–149.
- Reasenber, P. & Oppenheimer, D.H., 1985. FPFIT, FPLOT and FPPAGE; Fortran computer programs for calculating and displaying earthquake fault-plane solutions, Tech. rep., US Geological Survey.
- Reasenber, P.A., 1999. Foreshock occurrence before large earthquakes, *J. geophys. Res.*, **104**(B3), 4755–4768.
- Rey, J., Monfort Climent, D. & Tinard, P., 2016. Impact du séisme de 1799 sur le bâti courant des départements de Loire-Atlantique (44) et de Vendée (85), Brgm rapport final rp-66113-fr.
- Richter, C.F., 1935. An instrumental earthquake magnitude scale, *Bull. seism. Soc. Am.*, **25**(1), 1–32.
- Scotti, O., Baumont, D., Quenet, G. & Levret, A., 2004. The French macroseismic database SISFRANCE: objectives, results and perspectives, *Ann. Geophys.*, **47**(2–3), 571–581.
- Sellier, D., 2015. Le bassin de Grand-Lieu (Loire-Atlantique): relief et patrimoine géomorphologique, *Cahiers nantais*, **2015-2**, 57–75.
- Sibson, R.H., 1982. Fault zone models, heat flow, and the depth distribution of earthquakes in the continental crust of the United States, *Bull. seism. Soc. Am.*, **72**(1), 151–163.
- Small, E.E. & Anderson, R.S., 1998. Pleistocene relief production in Laramide mountain ranges, western United States, *Geology*, **26**(2), 123–126.
- Snyder, N.P., Whipple, K.X., Tucker, G.E. & Merritts, D.J., 2000. Landscape response to tectonic forcing: digital elevation model analysis of stream profiles in the Mendocino triple junction region, northern California, *Bull. geol. Soc. Am.*, **112**(8), 1250–1263.
- Stein, S., Liu, M., Camelbeck, T., Merino, M., Landgraf, A., Hintersberger, E. & Kübler, S., 2017. Challenges in assessing seismic hazard in intraplate Europe, *Geol. Soc., Lond., Spec. Publ.*, **432**(1), 13–28.
- Stucchi, M., *et al.*, 2013. The SHARE European earthquake catalogue (SHEEC) 1000–1899, *J. Seismol.*, **17**(2), 523–544.
- Tamaribuchi, K., Yagi, Y., Enescu, B. & Hirano, S., 2018. Characteristics of foreshock activity inferred from the JMA earthquake catalog, *Earth, Planets Space*, **70**(1), 90.
- Telbisz, T., Kovács, G., Székely, B. & Szabó, J., 2013. Topographic swath profile analysis: a generalization and sensitivity evaluation of a digital terrain analysis tool, *Zeitschrift für Geomorphologie*, **57**(4), 485–513.
- Ters, M. *et al.*, 1979a. Notice explicative de la carte géologique de la France au 1/50 000, feuille de Machecoul (XI-24), BRGM, Orléans, 36p.
- Ters, M. *et al.*, 1979b. Notice explicative de la carte géologique de la France au 1/50 000, feuille de l'Île-de-Noirmoutier. Pointe-de-St-Gildas (X-24-25), BRGM, Orléans, 36p.
- Ters, M. *et al.*, 1982. Notice explicative de la carte géologique de la France à 1/50 000, feuille de Saint-Philbert-de-Grand-Lieu (XII-24), BRGM, Orléans, 82p.
- Ters, M., Viaud, J., *et al.*, 1983. Notice explicative de la carte géologique de la France au 1/50 000, feuille de Challans (1125), BRGM, Orléans, 99p.
- Tessier, B., 2012. Stratigraphy of tide-dominated estuaries, in *Principles of Tidal Sedimentology*, pp. 109–128, Springer.
- Thion, I., Guennoc, P., Proust, J.-N., Mnier, D. & Leroy, P., 2007. Cartographie à 1/250000 de la plate-forme de Bretagne Sud : paléovallées quaternaires et structures du substratum, in *Congrès Association des Sédimentologistes Français*, Caen, France.
- Thion, I., Menier, D., Guennoc, P. & PROUST, J., 2008. Carte géologique au 1/250 000e de la marge continentale: Lorient (Bretagne Sud), Coordinateurs J.-N. PROUST et P. GUENNOC.—CNRS et BRGM.

- Traini, C., Menier, D., Proust, J.-N. & Sorrel, P., 2013. Transgressive systems tract of a ria-type estuary: the late holocene vilaine river drowned valley (France), *Mar. Geol.*, **337**, 140–155.
- Truffert, C., *et al.*, 2001. Levé géophysique aéroporté dans le Sud-Est du Massif armoricain (programme GéoFrance3D Armor2). Magnétisme et radiométrie spectrale, *Earth planet. Sci.*, **333**(5), 263–270.
- Van Vliet-Lanoë, B., *et al.*, 2009. Seismically induced shale diapirism: the Mine d'Or section, Vilaine estuary, Southern Brittany, *Int. J. Earth Sci.*, **98**(5), 969–984.
- Van Vliet-Lanoë, B., *et al.*, 2018. Middle Pleistocene seismically induced clay diapirism in an intraplate zone, western Brittany, France, *Quater. Res.*, **91**(1), 301–324.
- Vanne, J.-R., 1964. Géomorphologie sous-marine de la fosse du Croisic, *C.R. Acad. Sci.*, **258**, 2633–2636.
- Vavryčuk, V., 2014. Iterative joint inversion for stress and fault orientations from focal mechanisms, *J. geophys. Int.*, **199**(1), 69–77.
- Vignerresse, J., Jolivet, J., Cuney, M. & Bienfait, G., 1988. Etude Géothermique du Massif Armoricain, *Hercynica*, **4**(1), 45–55.
- Vignerresse, J.-L., 1988. La fracturation post-hercynienne du Massif Armoricain d'après les données de la géophysiques, *Géologie de la France*, **4**, 3–10.
- Wells, D.L. & Coppersmith, K.J., 1994. New empirical relationships among magnitude, rupture length, rupture width, rupture area, and surface displacement, *Bull. seism. Soc. Am.*, **84**(4), 974–1002.
- Whipple, K.X. & Tucker, G.E., 1999. Dynamics of the stream-power river incision model: implications for height limits of mountain ranges, landscape response timescales, and research needs, *J. geophys. Res.*, **104**(B8), 17 661–17 674.
- Wyns, R., 1986. Etude géoprospective du Massif Armoricain. Evolution tectonique de la partie Sud-Est du Massif Armoricain au Plio-Quaternaire: Essai de quantification des déformations et projection dans le million d'années venir., Rapport BRGM 86SGN100660.
- Wyns, R., 1991. Evolution tectonique du bâti armoricain oriental au Cénozoïque d'après l'analyse des paléosurfaces continentales et des formations géologiques associées, *Géologie de la France*, **3**(1), 1–42.
- Zonage Sismique de la France, 2011, Art. D. 563-8-1 du code de l'environnement, en vigueur depuis le 1er mai 2011.

## SUPPORTING INFORMATION

Supplementary data are available at [GJI](https://doi.org/10.1002/gji.12253) online.

**Catalogue.LRYON.docx**

**Catalogue.MACHE.docx**

**Catalogue.VENDE.docx**

**FM.MACHE.docx**

Please note: Oxford University Press is not responsible for the content or functionality of any supporting materials supplied by the authors. Any queries (other than missing material) should be directed to the corresponding author for the paper.

## APPENDIX A: SPARKER AND CHIRP RAW DATA AND SEISMIC FACIES DESCRIPTION IN THE BAIE DE BOURGNEUF

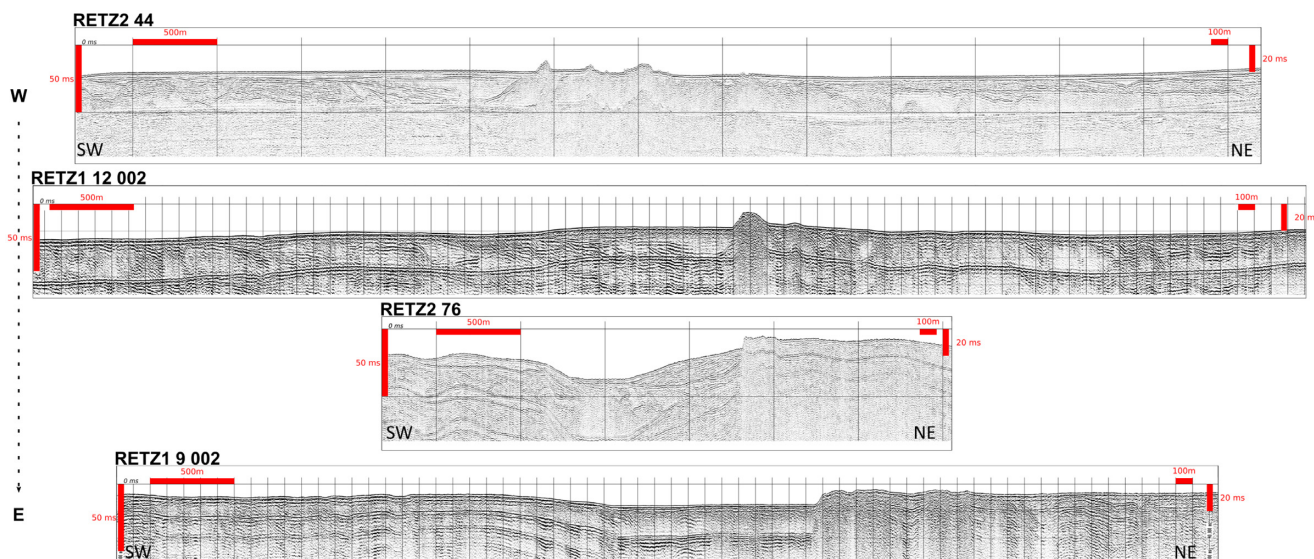


**Figure A1.** Sparker raw data for the representative samples of interpreted seismic profiles of RETZ1 and 2 cruises, with a 10-times vertical exaggeration (see Fig. 4 for profiles location and Fig. 8 for interpretation).

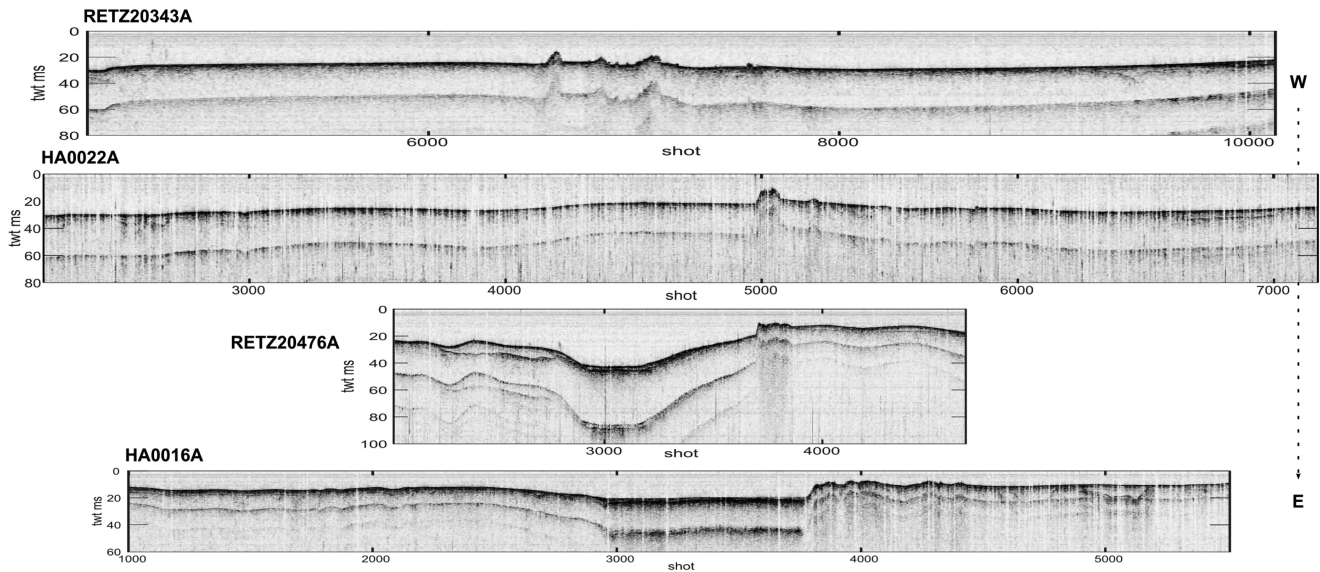


**Figure A2.** Chirp echo sounder raw data for the representative samples of interpreted seismic profiles of RETZ1 and 2 cruises, with a 10-times vertical exaggeration (see Fig. 4 for profiles location and Fig. 8 for interpretation).

Seismic Units	Internal configuration	Interpretation	Sparker illustration
Us1	chaotic stratification, oblique reflectors	Hercynian metamorphic and magmatic rocks	
Us2a	chaotic stratification, very low continuity of reflectors, transparent passes	Ypresian terrigenous deposits (sandstones and mudstones)	
Us2b	regular and subhorizontal stratification, vertical variation of amplitude	Lutetian-Bartonian bioclastic carbonates and carbonaceous sandstones	
U3a	wavy sub-horizontal to oblique moderately continuous reflectors	Sedimentary deposits	
U3b	tangential oblique geometry alternating with local slightly transparent-chaotic facies	Sedimentary deposits	
U4	subparallel, horizontal and continuous reflectors	Marine deposits	
Deaf acoustic facies	chaotic	Gas	

**Figure A3.** Description of the different acoustic units and facies encountered on Sparker seismic reflection profiles of RETZ1 and RETZ2 cruises (see Fig. 8 for profiles interpretation and Figs. A1 and A2 for raw profiles).

## APPENDIX B: EXTENDED STUDY OF BOUGUER ANOMALY IN THE VICINITY OF THE MACHECOUL FAULT USING GRAVITY MODELING

In the Marais Breton, the Bouguer anomaly values are quite homogeneous (Fig. B1a). South of the Machecoul Fault, the negative gravity anomaly of about 5 mGal is similar to anomalies found in other tertiary basins of NE Armorican Massif, ranging from 5 to 10 mGal (Wyns 1991; Jaeger 1967). One of them presenting a 12 mGal anomaly, has a 330 m thick of sediments deposited on the crystalline basement (Wyns 1991; Barbaroux *et al.* 1983). For others basins, Jaeger & Corpel (1967) estimate from modeling and slightly more severe anomalies that their infilling is about 500 m (Wyns 1991). According to the drill-holes data, the overall sediment thickness of the northern part of the Marais Breton is about 40 m, which is eight times less important than those basins, while the gravity anomaly of the Marais Breton (5 mGal) is only two times less (12 mGal). Considering the measurement points density provided by the BGI and therefore the Bouguer anomaly resolution, the signal of these small sedimentary thicknesses (up to 40 m) is likely too weak for the current heterogeneous coverage to record.

That is why we used a gravity modeling approach to study the consistency between the local infilling and the Bouguer anomaly in

the vicinity of the Machecoul Fault (Fig. B1b). In order to do that we constructed a 2-D density structure model of a fault-controlled sedimentary basin, constrained by the 05076X0005/SLM3 drill hole of the BSS database (Fig. B1c). The Machecoul Fault is represented as a vertical interface, separating two different nature blocks, with the NE compartment (footwall) consisting of crystalline basement (density of 2.8) and SW a sedimentary basin deposited on the base (density ranging from 1.53 to 2.1). The topography has also been taken into account in the upper part of the model to represent the slope fault. Then we computed its gravity response (Blakely (1995) method) and compared it to our Bouguer anomaly observed along a profile perpendicular to the fault (Fig. B1b). This profile extends to 10 km on either fault side, and the sampling rate is becoming lower near the fault (ranging from 1 km to 10 m, Fig. B1a).

Thus, even if the signal is very weak (around 5 mGal), its long-wavelength are compatible with the synthetic data computed with our 2-D model (Fig. B1c). There is therefore a good correlation with the infilling thickness found in the BSS drill holes considered in the vicinity of the Machecoul Fault. However, our reductive 2-D model cannot explain the very short wavelengths gravity signal along the profile, as well as the lateral variations along the fault. Indeed, these features are probably related to small subsurface heterogeneities.

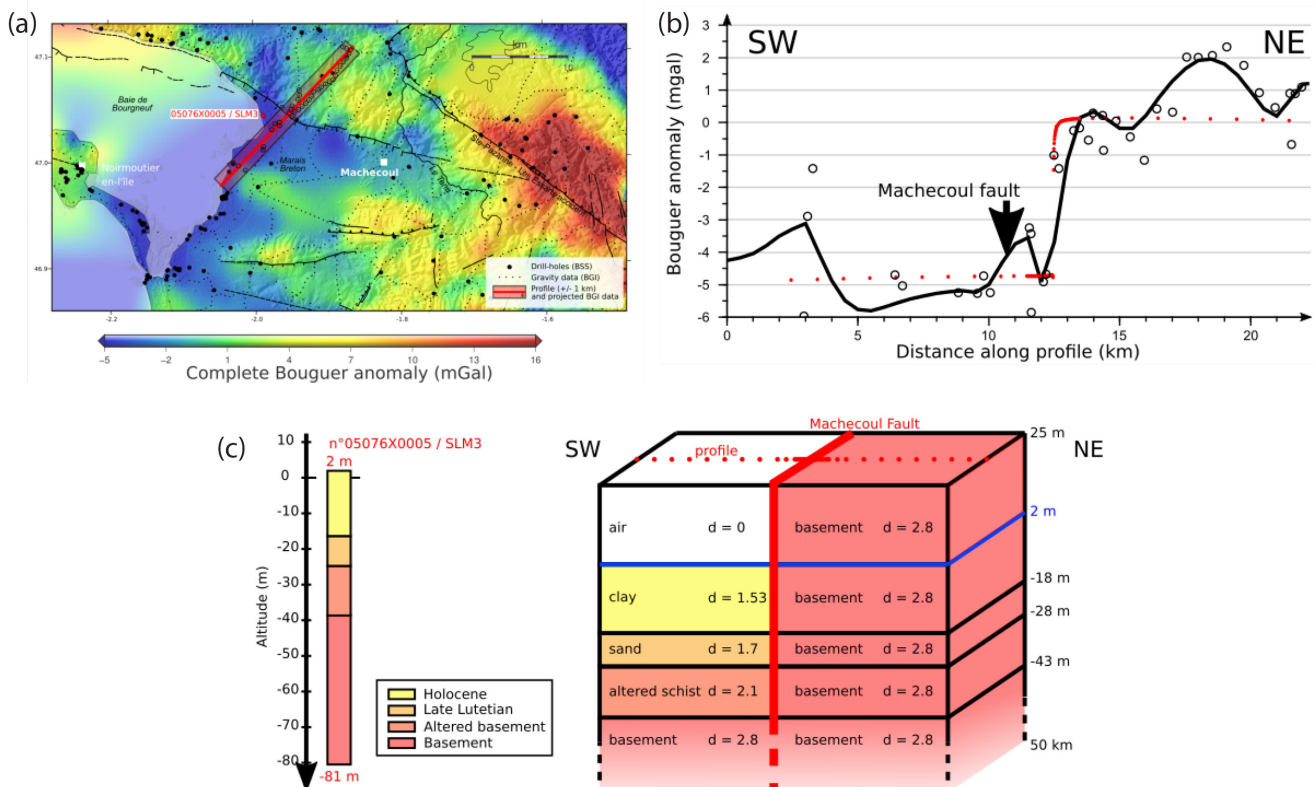


**Figure B1.** (a) Zoomed map (see Fig. 9 for the same map but bigger size) of complete Bouguer anomaly interpolation calculated from the free air anomaly provided by the BGI around Machecoul Fault. A slight white mask is applied to the offshore interpolation, considering the lack of data offshore. Small black circles are gravity data points from BGI, big black circles are drill holes from BSS used in this study. Red line is the profile and encircled small black circles are projected data points represented on the profile. (b) Profile. Small black circles are gravity data points from BGI. Calculated complete Bouguer anomaly response of our model (red dots) and observed complete Bouguer calculated from BGI data (black line). (c) 2-D density structure model of the Marais Breton and the Machecoul Fault in the considered area. The depths and densities of each layer were constrained by the 5076X0005/SLM3 drill hole (BSS) visible in (a).

## APPENDIX C: ADDITIONAL CONTENT ABOUT THE TEMPORARY LOCAL SEISMOLOGICAL EXPERIMENT MACHE

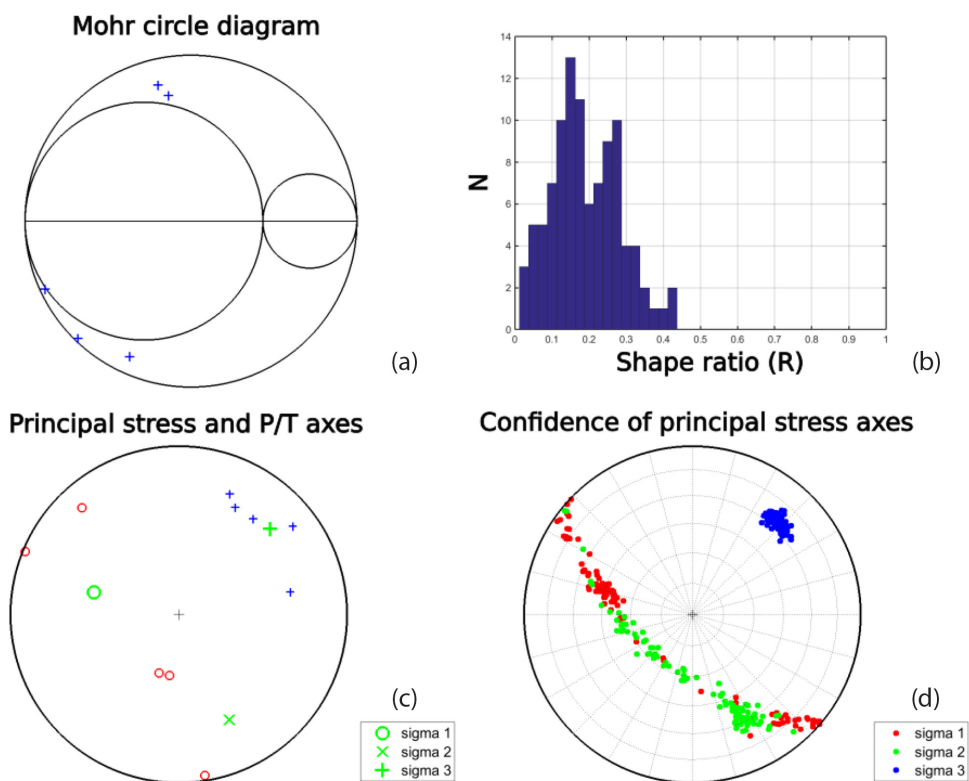


**Figure C1.** Stress inversion from fault plane solutions (Fig. 11b, except the n°27 focal mechanism) using the Vavryčuk (2014) method. (a) Mohr's circle diagram, (b) Histograms of the shape ratio  $R$ , (c)  $P/T$  axes and (d) Confidence limits of the principal stress directions.

APPENDIX D: NEOTECTONIC STRUCTURES IN WESTERN VENDÉE

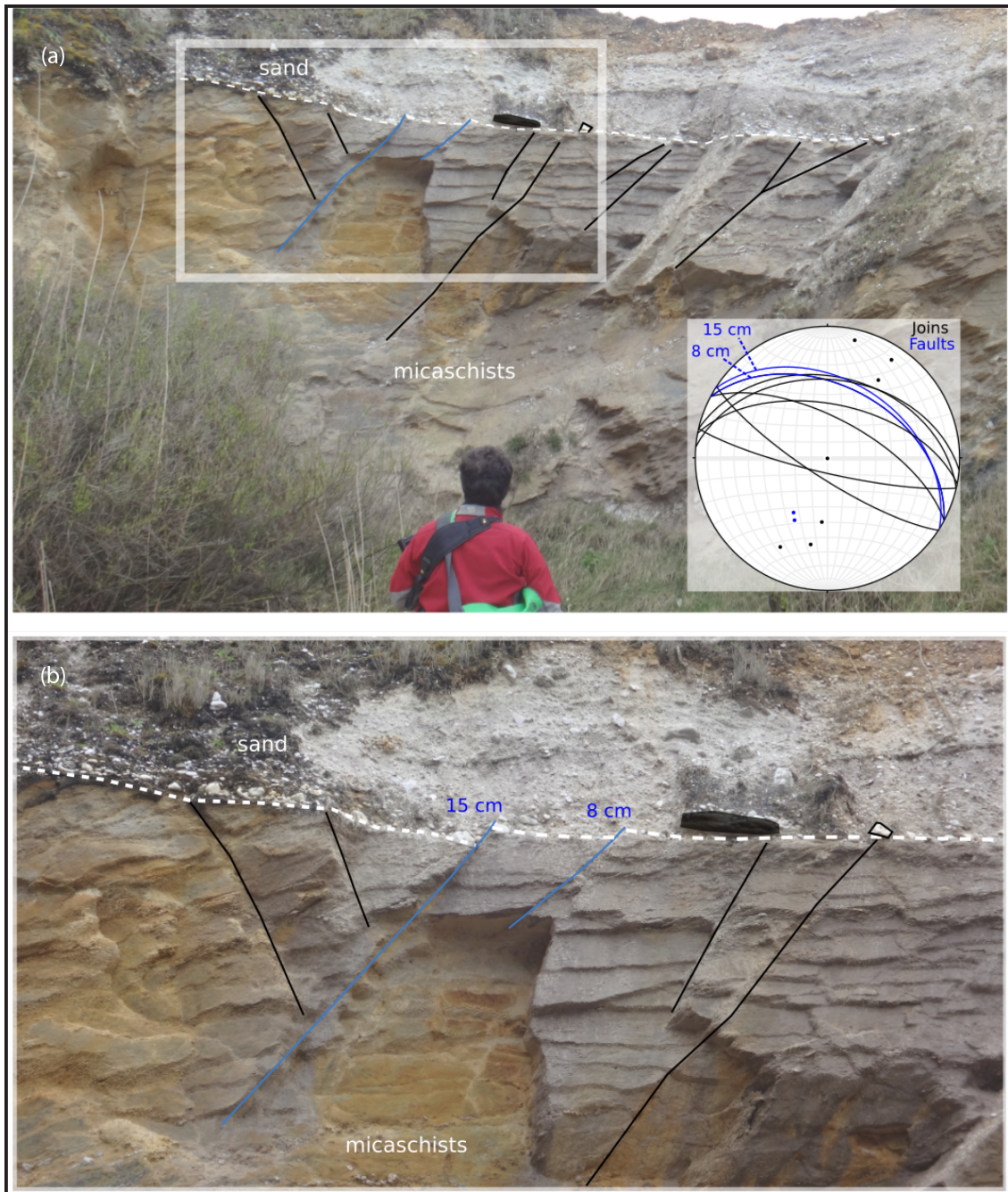


**Figure D1.** Illustrations of the corresponding outcrop and zoom on the small-scale purely dip-slip normal faults with throws and tension-shear joins, displacing a boulder level of unconstrained Pliocene to Quaternary age (white dashed line). Panel (b) corresponds to the zone framed in (a).